EXPLORING LYCOPODIACEAE ENDOPHYTES, *DENDROLYCOPODIUM* SYSTEMATICS, AND THE FUTURE OF FERN MODEL SYSTEMS

A Thesis

Presented to the Faculty of the Graduate School

Of Cornell University

In Partial Fulfillment of the Requirements for the Degree of

Master of Science

By

Alaina Rousseau Petlewski

May 2020

ABSTRACT

This thesis consists of three chapters addressing disparate topics in seed-free plant biology. Firstly, I begin to describe the endophyte communities of lycophytes by identifying the culturable endophytes of five Lycopodiaceae species. Microbial endophytes are integral factors in plant evolution, ecology, and physiology. However, the endophyte communities of all major groups of land plants have yet to be characterized. Secondly, I begin to re-evaluate the systematics of a historically perplexing genus, *Dendrolycopodium* (Lycopodiaceae). Lastly, I assess the status of developing fern model systems and discuss possible future directions for this work.

BIOGRAPHICAL SKETCH

Alaina was born in 1995 near Dallas, TX, but was largely raised in central California. In high school, she developed a love of plants and chemistry. She graduated summa cum laude from Humboldt State University in 2017 with a B.S. in botany and minor in chemistry. After graduating from Cornell, she plans to move back to the West Coast. She aspires to find a way to combine her love of plants and admiration for the arts, have a garden, be kind, share her knowledge, and raise poodles with her partner.

ACKNOWLEDGEMENTS

I would like to thank my advisor Fay-Wei Li and committee members Chelsea Specht and Robert Raguso, for their advisement on this work and for supporting me beyond my research pursuits by helping me to discover and act on what is right for me.

I would also like to thank the Bailey Hortorium staff, Anna Stalter and Peter Fraissinet, for all their help in coordinating loans and sampling herbarium materials. For providing *Dendrolycopodium* samples, I acknowledge and thank the following herbaria: University of Idaho Stillinger Herbarium; University of Montana Herbarium; New York Botanical Garden Steere Herbarium; University of Vermont Pringle Herbarium; Brown University Herbarium; and University of Washington Burke Herbarium. Additionally, thanks to Li-Yuong Kuo, Juan-Carlos Villareal, and Carl Rothfels for sending *Dendrolycopodium* samples.

Thank you to Paul Wolf for sending the barcoded adaptors for RAD-seq. I also extend my thanks to all of the BTI support staff, especially Doug Carruthers and Gary Hovarth for supplying me with the necessary materials for my research.

Thank you to Cornell's Plant Biology department for their support through teaching assistantships, which not only funded me but gave me invaluable teaching experience. Thank you to my research funding sources: Society for the Study of Evolution R.C. Lewontin Early Award; American Society of Plant Taxonomists Graduate Student Research Award; and the Andrew W. Mellon Student Research Grant. The microbiome studies would have been a near impossible undertaking without the meticulous dedication of Ariel Patterson—thank you so much for all

your help and patience with the bacterial culturing. None of this work would have been possible without mentorship from Jessica Nelson and Duncan Hauser. I am incredibly grateful to them for their help with experimental design and data analysis, but more importantly, their friendship.

Furthermore, I am so thankful for the friends and mentors who, over the years, have shaped me by sharing their joy, wisdom, and love: Nikole Rubner, Jessica Chu, Marissa Lopez, Corinne Webb, Bailey Timmons, Kjirsten Wayman, Marie Antoine, Mihai Tomescu (and co.), Michael Mesler, Courtney Otto, and all those I'm sure I forgot. I am incredibly grateful to the innumerable writers, artists, musicians, and creators who have enriched even the darkest points in my life with beauty and empathy. Finally, I cannot adequately express the gratitude I feel towards my partner Rachael, my parents, my sister Leiana, and my dogs Shinka and Remy. I love you all so much.

TABLE OF CONTENTS

LIST OF FIGURES

LIST OF TABLES

CHAPTER ONE

CHARACTERIZING THE CULTURABLE MICROBIOME OF FIVE LYCOPODIACEAE SPECIES

1.1 Introduction

Every macro-organism lives in close association with countless micro-organisms and plants are no exception. Some plant symbionts, such as arbuscular mycorrhizal fungi (AMF), are considered critical in the establishment of early land plants and their continued success (Heckman et al., 2001; Taylor and Krings, 2005; Delaux et al., 2012; Selosse et al., 2015). Meanwhile, many plants harbor nitrogen-fixing bacteria, like *Rhizobium*, *Frankia*, and *Nostoc*, which not only influence plant growth, but the surrounding environment (Santi *et al*., 2013).

Yet, these well-known specialized symbioses are not the only ones that impact plant growth and ecological interactions. In fact, communities of bacteria, archaea, fungi, and other eukaryotic microbes can live within healthy plant tissues (Berg *et al*., 2016). These plant endophyte communities are often highly diverse, even within the same host species and geographic location (Higgins *et al*., 2007; U'Ren *et al*., 2010; Nelson and Shaw, 2019). This diversity is reflected in the various roles these endophytes fill within their host plant— they may be mutualistic, commensalistic, pathogenic, latently saprotrophic, and may act to influence plant growth and interactions with other organisms, including pathogens (Porras-Alfaro and Bayman, 2011). Thus, plant-microbial interactions are undoubtedly underestimated but integral factors in shaping ecosystem structuring (Rudgers *et al.,* 2003; Afkhami and Strauss, 2016; Aguilar-Trigueros and Rillig, 2016).

Regardless of their importance, microbiomes have not been well characterized for all major lineages of land plants. Studies on the microbiomes of the club mosses (Lycopodiaceae) are relatively scarce, and those that do exist largely employ light microscopy to morphologically classify fungal hyphae into broad categories (Freeberg 1962; Duckett and Ligrone, 1992; Schmid and Oberwinkler, 1993; Fernandez *et al*., 2008; Kessler *et al.*, 2010a, b; Zubek *et al.*, 2010; Muthukmar and Prabha, 2013; Lehnert *et al*., 2017). Studies which have fully isolated and characterized endophytes in this group have yielded some broadly applicable and thought-provoking results. Zhu *et al.* (2010) discovered a novel fungal endophyte of *Huperzia serrata* which produces huperzine A, a bioactive compound of interest in treating Alzheimer's disease. Other studies indicate that some, but not all members, of this family do not all host vital AMF associations (Harley and Harley, 1987; Gemma *et al.*, 1992; Treu *et al*., 1996; Winther and Friedman, 2008; Zhao, 2000). Instead, they may host higher abundances of ascomycetes and basidiomycetes (Benucci *et al.,* 2020). This study aims to expand knowledge of lycophyte microbiomes by characterizing and comparing the culturable endophytic fungi and bacteria in five Lycopodiaceae species found in central New York.

1.2 Methods

1.2.1 Plant collection location

Huperzia lucidula, Spinulum annotinum, Lycopodium clavatum, Diphasiastrum digitatum, and *Dendrolycopodium dendroideum* were collected from a sympatric population in Shindagin Hollow State Forest (42.33707, -76.33905).

Aerial and subterranean tissues from one plant of each species were collected once a week, for four consecutive weeks, in June 2019 (6/4, 6/10, 6/17, 6/24).

1.2.2 Plant sampling & endophyte isolation

Intact plants were brought to the lab and refrigerated until they could be cleaned and processed (no more than 48 hours after collection). They were rinsed with deionized (DI) water to remove large debris. Plants were divided into three categories of tissue: aerial; subterranean shoot; and subterranean root. Each tissue type was transferred to a sterile hood, rinsed again in sterile DI water to remove finer debris, and chopped into $2mm^2$ segments. Segments were surface sterilized by submerging them in 95% ethanol for 30 seconds, 10% bleach (with a few drops of 1% Tween 20) for two minutes, and 70% ethanol for two minutes (based on Arnold, 2002). Segments were allowed to air dry under sterile air on autoclaved filter paper. These protocols have been shown to eliminate epiphytic microbes (Schulz *et al.,* 1993; Arnold, 2002), but to ensure this, one piece from each batch was rubbed on lysogeny broth (LB) and 1.5% malt extract agar (MEA) plates. If anything grew on the control plate, the entire batch was disregarded as contaminated. For each sample, ten segments of aerial tissue, five segments of subterranean shoot, and five segments of subterranean root were plated out onto each type of media. Plates were sealed with parafilm, left at room temperature, and regularly checked for growth. Subcultures were made to separate different morphologies.

1.2.3 Culture identification

Fungi— Once pure cultures were obtained, hyphal samples from each culture were transferred into a 2mL tube with 1.5% malt extract broth (MEB) and allowed to

grow. Once growth was observed, tubes were centrifuged for 2 minutes at 2100G and the media was removed. Two sterile 3.5mm stainless steel balls were added to each tube. Tubes were then submerged in liquid nitrogen and shaken at 1500 strokes per minute for one minute on a MiniG 1600 (SPEX Sample Prep). DNA was extracted following a modified CTAB protocol (Saghai-Maroof *et al*., 1984; Appendix 1). Extracts were amplified using ITS1f (Gardes and Bruns, 1993) and LR3 (Vilgalys and Hester 1990) primers (see Appendix 2). Successful products were cleaned with an ExoSAP protocol (New England BioLabs) and sent to Eurofins for Sanger sequencing. Forward and reverse Sanger sequences were joined using Geneious Prime (Version 2019.2.1) and compared to the NCBI GenBank database using BLAST searches. Species names were assigned if sequences matched to only one species with at least 97% identity and full coverage. Unidentifiable taxa were grouped together if sequences were at least 97% similar (VSEARCH, Rognes *et al.,* 2016) and given an identifier based on higher level taxonomic ranks.

Bacteria— Once pure cultures were obtained, a sterile pipet tip was used to transfer bacteria into a 0.2 mL tube for colony PCR with 27F (Lane *et al*., 1991) and 1492Rl (Turner *et al.*, 1999) primers (Appendix 3). If colony PCR failed, DNA extractions were carried out based on Wilson, 2001 (Appendix 4) and subject to the same PCR protocol as above. All successful amplification products were cleaned using an ExoSAP protocol (New England BioLabs). Clean PCR products were submitted to Eurofins for Sanger sequencing. Forward and reverse Sanger sequences were joined using Geneious Prime (Version 2019.2.1) and compared to the NCBI GenBank database using BLAST searches. Species names were assigned

if sequences matched to only one species with at least 97% identity and full coverage. Unidentifiable taxa were grouped together if sequences were at least 97% similar (VSEARCH, Rognes *et al.,* 2016) and given an identifier based on higher level taxonomic ranks.

1.3 Results

1.3.1 Fungi

Of the 800 plates started, five were discarded as contaminated (all from *De. dendroideum* subterranean stem) and 76 grew fungi (9.5% culture rate), of which 46 were identified (5.75% isolation rate; Table 1.1). These 46 cultures belong to 15 distinct species (Table 1.2, Figure 1.1, Appendix 5), and 5 were unidentifiable to any existing taxonomic group. Only four species were isolated more than once. Most species represent Ascomycota, with the exception of two Mucoromycota representatives and one Basidiomycota. *H. lucidula* and *S. annotinum* had the greatest culture number and species richness, followed by *De. dendroideum*, *L. clavatum*, and *Di. digitatum* (which only yielded one culture). Of the 46 cultures, 22 cultures from *S. annotinum* aerial tissue were identified as Dothideomycetes sp. 1.

1.3.2 Bacteria

Of the 800 plates started, 161 plates grew bacteria (20.1% culture rate), of which 157 were identified (19.6% isolation rate; Table 1.3, Appendix 6). These 157 cultures belonged to 52 distinct species (Table 1.4, Figure 1.2) in 17 families (Figure 1.3). 23 species were isolated more than once. *H. lucidula* had the greatest culture number and species richness, followed by *S. annotinum*, *L. clavatum, Di. digitatum*, and *De. dendroideum.* Although aerial tissue had the lowest number of cultures, it

had a higher richness than either subterranean shoots or roots, owing to the high richness in *H. lucidula* aerial tissue.

Table 1.1 Number of cultures identified from each plant species and tissue type

	Aerial shoot	Subterranean shoot	Subterranean root	TOTAL
De. dendroideum	2	3	1	6
Di. digitatum	0	1	0	1
H. lucidula	3	3	1	7
L. clavatum	3	0	1	4
S. annotinum	26	2	0	28
TOTAL	34	9	3	46

Table 1.2 Number of fungal species identified from each plant species and tissue type

	Aerial shoot	Subterranean shoot	Subterranean root	TOTAL
De. dendroideum	2	1	1	4
Di. digitatum	0	1	0	1
H. lucidula	3	3	1	7
L. clavatum	2	0	1	3
S. annotinum	5	2	0	7
TOTAL	8	3	3	15

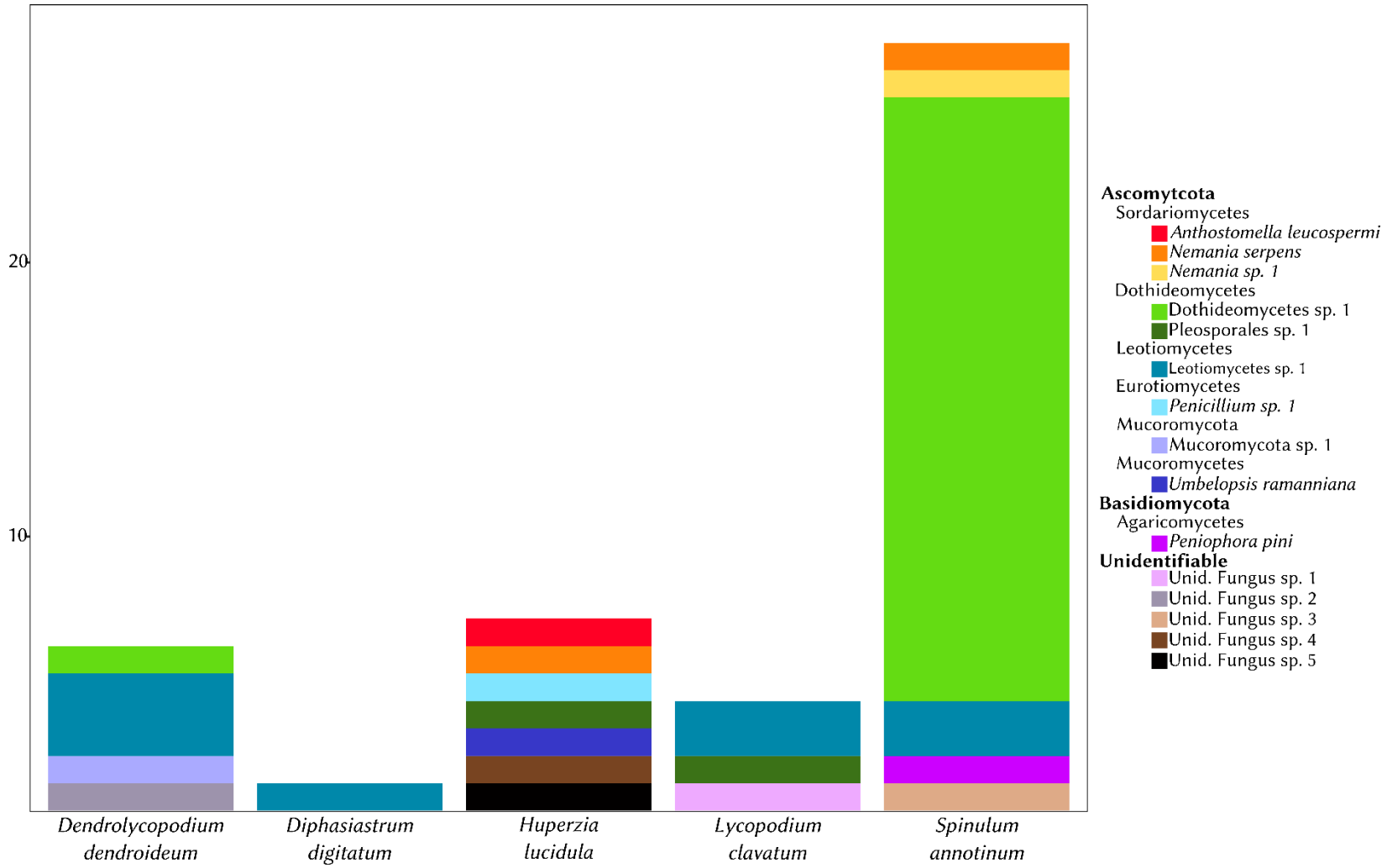

Figure 1.1 Fungal species found in each plant species. Unid. = unidentifiable. For OTU table, see Appendix 6

Table 1.3 Number of cultures identified from each plant species and tissue type

	Aerial shoot	Subterranean shoot	Subterranean root	TOTAL
De. dendroideum	1	10	4	15
Di. digitatum	2	7	12	21
H. lucidula	29	20	5	54
L. clavatum	3	0	21	24
S. annotinum	10	14	19	43
TOTAL	45	51	61	157

Table 1.4 Number of bacterial species identified from each plant species and tissue type

	Aerial shoot	Subterranean shoot	Subterranean root	TOTAL
De. dendroideum	1	7	4	9
Di. digitatum	2	5	8	12
H. lucidula	22	14	4	34
L. clavatum	2	0	14	15
S. annotinum	7	7	9	17
TOTAL	29	24	23	52

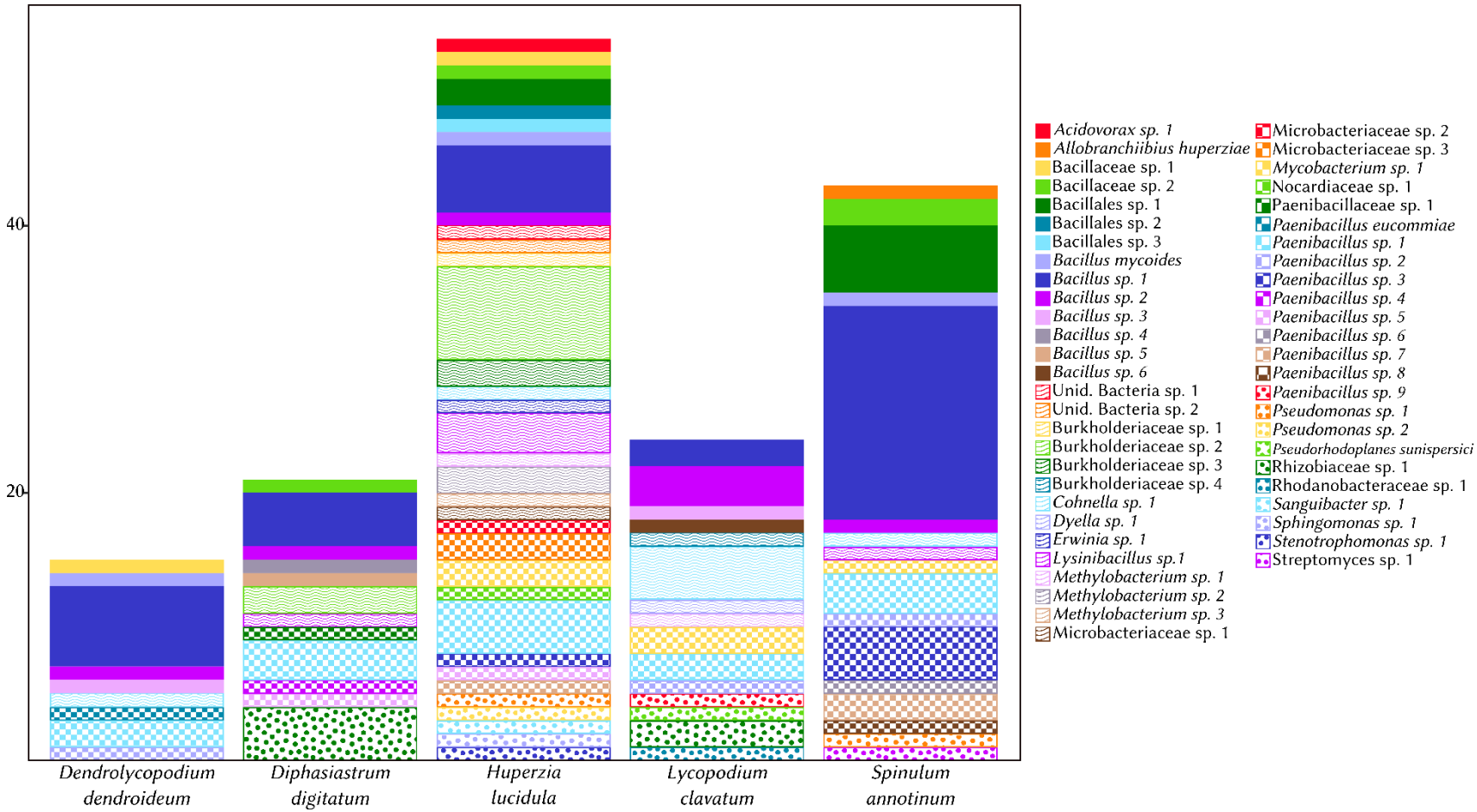

Figure 1.2 Bacterial species found in each plant species. Unid. = unidentifiable. For OTU table, see Appendix 5

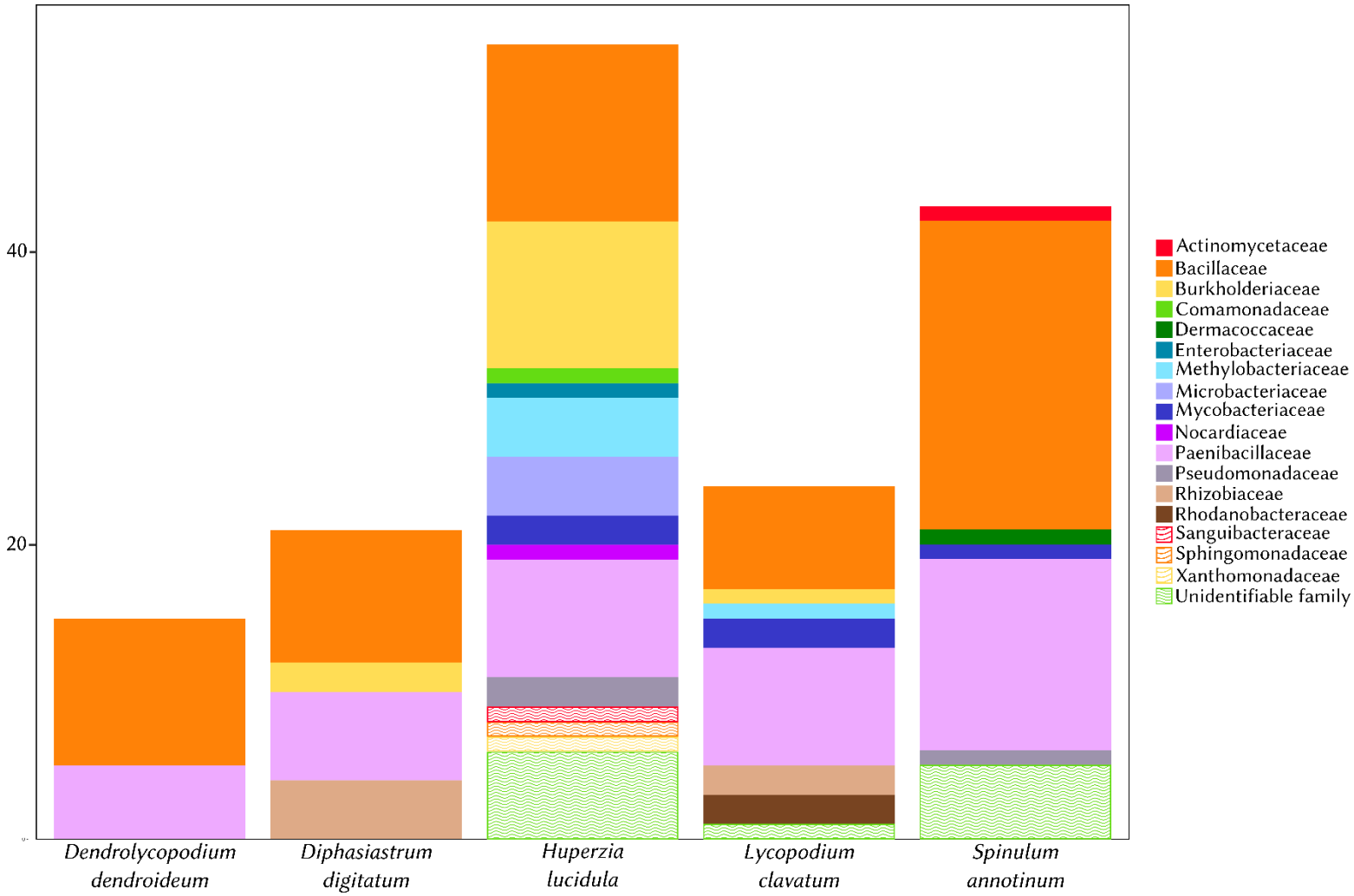

Figure 1.3 Bacterial families found in each plant species

1.4 Discussion

1.4.1 Fungal culturing rate and community composition

In this study, 9.5% of the 800 surface sterilized plant segments grew fungi. Using the same methods, Nelson and Shaw (2019) observed fungal growth in 14.5% of surface sterilized *Marchantia polymorpha* fragments. When conducting a similar study on *Huperzia serrata* in China, Wang *et al.* (2016) observed a 61.1% fungal culture rate. Another study on the aerial tissue of *L. clavatum* and *S. annotinum* in Poland yielded a 72.2% culture rate (Pawlowska *et al.,* 2014). However, culture rates are known to vary greatly—from <1% to 41% in boreal and arctic systems to up to 90% in tropical leaves (Higgins *et al.,* 2007; Lodge *et al.,* 1996; Porras-Alfaro and Bayman, 2011). Additionally, it stands to reason that even subtle differences in surface sterilization methods and culture conditions can yield vastly different culture rates. While the studies by Wang *et al.* (2016) and Pawlowska *et al.* (2014) used similar methods and employed the same negative controls, their methods and media types were not identical to those used for this study.

Despite the high culture rate, Pawlowska *et al.* (2014) only identified 18 distinct taxa, all of which were ascomycetes, with representatives from the class Dothideomycetes isolated most frequently. This is similar to the data presented here, in which 25 of 46 cultures represented Dothideomycetes (2 distinct species). Likewise, most of the fungi identified by Wang *et al.* (2016) were ascomycetes, mostly representing the class Sordariomycetes, followed by Dothideomycetes. Both classes were observed in this study. They also observed a small portion of isolates representing Eurotiomycetes (observed here), Leotiomycetes (observed here),

Orbiliomycetes, and Pezizomycetes, as well as some members of Basidiomycota (Agaricomycetes, also observed here). Neither study reports finding members of Mucoromycota, but they were observed in this study.

Five of the seven fungal taxa identified in *H. lucidula* were only found in *H. lucidula.* Furthermore, fungi common to other samples, like Leotiomycetes sp. 1, were not isolated from *H. lucidula* (Figure 1.1; Appendix 5). Thus, the fungal endophyte community composition of *Huperzia* may be distinct from other members of Lycopodiaceae sampled. *Huperzia* belongs to a different subfamily (Huperzioideae) than the other species sampled in this study (Lycopodioideae) (Figure 1.4). Further studies utilizing next generation amplicon-sequencing (such as that executed by Benucci *et al.,* 2020) on broad geographic and phylogenetic collections of Lycopodiaceae could explore potential correlations between the plant phylogenetic relationships and endophyte community compositions.

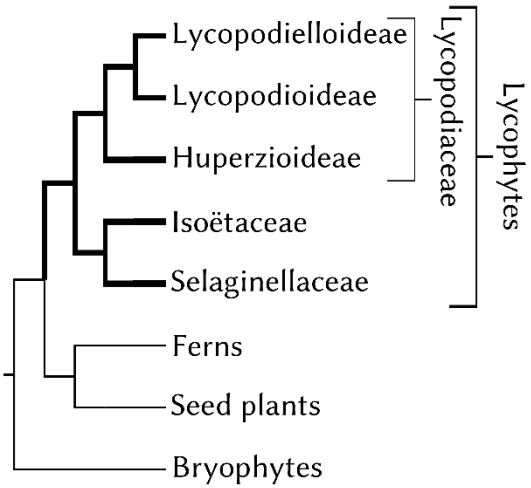

Figure 1.4 Phylogeny of Lycopodiaceae subfamilies. *H. lucidula* represents Huperzioideae; *De. dendroideum, Di. digitatum, L. clavatum,* and *S. annotinum* represent Lycopodioideae. (PPG I, 2016)

1.4.2 Potential roles of isolated fungal endophytes

Without functional studies, it is impossible to determine where these fungal-lycophyte symbioses fall on the scale from mutualism to parasitism/pathogenicity, and the possibility of commensalism should not be underestimated. However, the metabolic characteristics of some of the fungi identified in this study have been previously described. For example, *Nemania serpens* produces compounds known as nemanifuranones, which are a series of 5-alkenyl-3(2H)-furanones with a rare C2 hemiacetal with short alkyl chains. Nemanifuranone A, in particular, has been found to exhibit growth inhibition of both gram-positive and gram-negative bacteria. Thus, this species may act to limit bacterial infection (Ibrahim *et al.*, 2017). Contrarily, the two plants in this study from which *Nemania spp.* were isolated also had the highest culture rate of bacteria. Further testing would be needed to explore this potential interaction.

In addition to *Nemania,* an unknown *Penicillium* species was isolated from *H. lucidula* in this study. Previous studies indicate that *Penicillium spp.* may contribute to salinity stress resistance and promote growth under abiotic stress in soybean (Khan *et al.,* 2011; Khan and Lee, 2013). *Peniophora pini,* found here in *S. annotinum,* is a pathogen that causes white pocket rot in many species of pine, but it is also antagonistic to other conifer pathogens (Ayer *et al.,* 1995). Its presence and potential role in other plants has not been described.

Furthermore, *Umbelopsis spp.* produce metabolically relevant fatty acids, including oleic, linoleic, and arachidonic acids (Grantina-Ievina *et al.,* 2014), though it is not known if these might impact a host plant. It should be noted that

Mucoromycota includes many representatives which interact with most groups of land plants, including the mutualist AMF (Glomeromycotina). In fact, a nutritional mutualism has been described between *Lycopodiella inundata* and Mucoromycotina fine root endophytes (Hoysted *et al*., 2019). However, Mucoromycota also includes some saprobes and pathogens (Bonfante and Venice, 2019). Thus, the nature of the interaction between *Umbelopsis raminiana* and the unidentifiable Mucoromycota sp. 1, isolated from *H. lucidula* and *De. dendroideum* respectively, would be good early targets for functional analyses, especially since it is unknown if these plants harbor AMF symbioses.

The potential role of *Anthostomella leucospermi* is unknown. Furthermore, given the breadth of taxa included in the remaining groups (Leotiomycetes, Dothideomycetes, and unidentifiable fungi), it is difficult to speculate as to their potential roles.

1.4.3 Bacterial culturing rate and community composition

In this study, 20.1% of the 800 surface sterilized plant segments grew bacteria. No studies exist which explore the culturable bacterial endophyte communities of Lycopodiaceae, and a canvassing of studies conducted on other plants revealed a distinct lack of reporting of bacterial culture rates. Thus, it is difficult to determine 20.1% represents a relatively high or low culture rate. Benucci *et al.* (2020) used next-generation amplicon-sequencing techniques to characterize the bacteria growing in association with Lycopodiaceae roots in New Zealand. They describe only 515 bacterial OTUs. However, their experimental design is significantly different from this study, as they did not surface sterilize their samples.

Therefore, it would be unreasonable to use as a benchmark for the results of our study.

1.4.4 Potential roles of isolated bacterial endophytes

Like fungal endophytes, bacterial endophytes can have a wide range of effects on their plant hosts, but specific functional studies are needed to accurately describe the interactions between lycophytes and their endophytes. However, speculation can be made based on previously described interactions. For example, *Bacillus mycoides* may act to control pathogens in sugar beets (Bargabus *et al.,* 2002). Yet, for the many other unidentifiable *Bacillus spp*., Bacilliaceae spp., and Bacilliales spp. isolated in this study, it is impossible to hypothesize as to how they may impact their hosts. The same is true for the numerous unidentifiable *Paenibacillus spp.,* Panabacilliaceae, Microbacteriaceae, Nocardiaceae, and Rhodanobacteriaceae.

Some *Pseudomonas spp.* promote plant growth via multiple mechanisms, including auxin production and increasing phosphate and nitrogen availability (Gnanamanickman, 2007; Oteino *et al.,* 2015). Similarly, there is evidence that some species of *Cohnella*, *Lysinibacillus,* and Burkholderiaceae promote plant growth either through phytohormone production or by increasing nutrient availability (Niang *et al.,* 2018; Gnanamanickman, 2007; Naureen *et al.,* 2017; Shabanamol *et al.,* 2017). Meanwhile, many *Acidovorax spp.* and *Erwinia spp.* are pathogens (Gnanamanickman, 2007). Finally, *Sanguibacter spp.* may increase resistance to cadmium (Rajkumar *et al.,* 2009).

Two genera isolated here are of particular interest as lycophyte symbionts: *Methylobacterium* and *Allobranchiibius*. Like some of the other bacterial taxa described above, *Methylobacterium* spp. may impact plant growth by producing phytohormones (like cytokinins and auxins) and increasing nitrogen availability (Holland, 1997; Kutschera, 2007). Additionally, *Methylobacterium spp.* have been hypothesized to be ubiquitous co-evolving symbionts across the land plant phylogeny (Holland, 1997). This hypothesis warrants further investigation. *Allobranchiibius* is represented by a single species, *A. huperziae,* isolated from *Huperzia serrata* roots in China (Ai *et al*., 2017). Its activity in lycophytes is unknown, however it was found in *S. annotinum* aerial tissue in this study. Given that it has only been reported as a lycophyte endophyte, in two geographically disparate studies, the possibility of host-specificity should be investigated.

1.4.5 Limitations of this study

Any study on culturable endophyte communities inherently carries significant bias. Firstly, microbial species abundances have limited, if any, meaning. For instance, in this study, *S. annotinum* exhibited significant growth of Dothideomycetes sp. 1 and *Di. digitatum* only yielded one fungal culture. It is entirely possible that this is reflective of the fungal communities in these plants. However, it is also possible that Dothideomycetes sp. 1 grew exceptionally well in this study's growth conditions, while the fungal endophytes in *Di. digitatum* found this to be uninhabitable. Thus, it is impossible to make confident conclusions regarding diversity indices and other statistical analyses. Secondly, the low number of cultures in this study did not allow for statistical analyses. Finally, because AMF

are obligate symbionts, they cannot be cultured and thus would have been impossible to identify with this experimental design.

1.4.6 Future directions

This culture data, while a valuable first step in characterizing microbial endophyte communities, needs to be accompanied by a next-generation amplicon-sequencing (amplicon-seq) data set to more thoroughly characterize the complete endophyte community. The cultures from this study could be used to create a mock community to act as a control for unequal amplification biases in the amplicon-seq data. Additionally, an amplicon-seq study could assess if AMF are present through the use of a paired primer set (SSUmCf-LSUmBr and SSUmAf-LSUmAr; Kruger *et al.,* 2012). Nelson and Shaw (2019) reported 90 species identified from their *M. polymorpha* endophyte cultures, compared to 883 from the ITS amplicon-seq data set. I suspect that the results of an amplicon-seq study on Lycopodiaceae would similarly yield a far greater number of both fungal and bacterial OTU's, as well as more reliable species abundance data. The increase in statistical power inherent in amplicon-seq data sets, coupled with expanded sampling, would also allow to explore questions of host and tissue specificity.

Furthermore, to fully characterize the microbiome of these plants, the unidentifiable OTU's from this study need to be fully described and given taxonomic assignment. Then, large scale functional assays on all OTU's are needed to determine how these endophytes interact with both their host plant and each other. These endophytes and their exudates may also possess utility in other applications, such as pest/pathogen management in agriculture or pharmaceutical development.

REFERENCES

Afkhami, M.E. and S.Y. Strauss. 2016. Native fungal endophytes suppress and exotic dominant and increase plant diversity over small and large spatial scales. Ecology 97(5):1159-1169.

Aguilar-Trigueros, C.A. and M.C. Rillig. 2016. Effect of different root endophytic fungi on plant community structure in experimental microcosms. Ecology and Evolution 6(22):8149--8158.

Ai, M-J., Y. Sun, H-M Sun, H-Y. Liu, L-Y. Yan, and Y-Q. Zhang. 2017. *Allobranchiibius huperziae* gen. nov, sp. nov., a member of Dermacoccaceae isolated from the root of a medicinal plant *Huperzia serrata* (Thunb.). International Journal of Systematic and Evolutionary Microbiology 37: 4210-4215.

Arnold, A.E. 2002. Neotropical fungal endophytes: diversity and ecology. PhD diss., University of Arizona.

Ayer, W.A., D.J. Muir, and P. Charkrawarty. 1995. Phenolic and other metabolites of *Phellinus pini*, a fungus pathogenic to pine. Phytochemistry 42(5): 1321-1324.

Bargabus, R.L., N.K. Zidack, J.E. Sherwood, and B.J. Jacobsen. 2002. Characterisation of systemic resistance in sugar beet elicited by a non-pathogenic, phyllosphere-colonizing *Bacillus mycoides*, biological control agent. Physiological and Molecular Plant Pathology 61(5): 289-298.

Benucci, G. M. N., D. Burnard, L. D. Shepherd, G. Bonito, and A. B. Munkacsi. 2020. Evidence for co-evolutionary history of early diverging Lycopodiaceae plants with fungi. Frontiers in Microbiology 10.

Berg, G., D. Rybakova, M. Grube, and M. Köberl. 2016. The plant microbiome explored: Implications for experimental botany. Journal of Experimental Botany 67:995–1002.

Bonfante, P. and F. Venice. 2019. Mucoromycota: going to the roots of plant-interacting fungi. Fungal Biology Reviews, *In Press*.

Delaux, P. M., A.K. Nanda, C, Mathé, N. Sejalon-Delmas, and C. Dunand. 2012. Molecular and biochemical aspects of plant terrestrialization. Perspectives in Plant Ecology, Evolution, and Systematics 14:49–59

Duckett, J. and R. Ligrone. 1992. A light and electron microscope study of the fungal endophytes in the sporophyte and gametophyte of *Lycopodium cernuum* with observations on the gametophyte-sporophyte junction. Canadian Journal of Botany 70:58--72.

Fernández, N., M. Messuti, and S. Fontenla. 2008. Arbuscular mycorrhizas and dark septate fungi in *Lycopodium paniculatum* (Lycopodiaceae) and *Equisetum bogotense* (Equisetaceae) in a Valdivian Temperate Forest of Patagonia, Argentina. American Fern Journal 98:117–127.

Freeberg, J. 1962. Lycopodium prothalli and their endophytic fungi as studies in vitro. American Journal of Botany 49:530--535.

Gardes, M. and T.D. Bruns. 1993. ITS primers with enhanced specificity for basidiomycetes-application to the identification of mycorrhizae and rusts. Molecular ecology 2(2):113--118.

Gemma, J. N., R.E. Koske, and T. Flynn. 1992. Mycorrhizae in Hawaiian pteridophytes: occurrence and evolutionary significance. American Journal of Botany 79:843–852.

Gnanamanickam, S.S. (eds.). 2007. *Plant-Associated Bacteria.* Springer, Dordrecht.

Harley, J. L. and E.L. Harley. 1987. A check-list of mycorrhiza in the British Flora. New Phytologist 105:1–102.

Heckman, D. S, D.M. Geiser, B.R. Eidell, R.L. Stauffer, N.L. Kardos, and S.B Hedges. 2001. Molecular evidence for the early colonization of land plants by fungi and plants. Science 293:1129–1133.

Higgins, K. L., A.E. Arnold, J. Miadlikowska, S.D. Sarvate, and F. Lutzoni. 2007. Phylogenetic relationships, host affinity, and geographic structure of boreal and arctic endophytes from three major plant lineages. Molecular Phylogenetics and Evolution 42:543–555.

Holland, M.A. 1997. *Methylobacterium* and plants. Recent Developments in Plant Physiology 1: 207-213.

Hoysted, G.A., A. S. Jacob, J. Kowal. P. Giesemann, M.I. Bidartondo, J.G. Duckett, G. Gerbauer, W.R. Rimington, S. Schornack, S. Pressel, and K. J. Field. 2019. Mucoromycotina fine root endophyte fungi form nutritional mutualisms with vascular plants. Plant Physiology 181: 565-577.

Ibrahim, A., D. Sorensen, H.A. Jenkins, L. Ejim, A. Capretta, M.W. Sumarah. 2017. Epoxynemanione A, nemanifuranones A-F, and nemanilactones A-C, from *Nemania serpens*, an endophytic fungus isolated from Riesling grapevines. Phytochemistry. 140: 16-26.

Kessler, M., R. Jonas, D. Cicuzza, J. Kulge, K. Piatek, P. Naks, and M. Lehnert. 2010a. A survey of the mycorrhization of Southeast Asian ferns and lycophytes. Plant Biology 12:788–793.

Kessler, M., R. Jonas, D. Strasberg, and M. Lehnert. 2010b. Mycorrhizal colonizations of ferns and lycophytes on the island of La Réunion in relation to nutrient availability. Basic Applications in Ecology 11:329–336.

Khan, A.L. and I-J. Lee. 2013. Endophytic *Penicillium funiculosum* LHL06 secretes gibberellin that reprograms *Glycine max* L. growth during copper stress. BMC Plant Biology 13: 86.

Khan, A.L., M. Hamayun, N. Ahmad, J. Hussain, S-M. Kang, Y-H. Kim, M. Adnan, D-S. Tang, M. Waqas, R. Radhakrishman, Y-H. Hwang, and I-J. Lee. 2011. Salinity stress resistance offered by endophytic fungal interaction between *Penicillium minioluteum* LHL09 and *Glycine max* L. Journal of Microbiology and Biotechnology 21(9): 893-902.

Kruger, M., C. Kruger, C. Walker, H. Stockinger, A. Schussler. 2012. Phylogenetic reference data for systematics and phylotaxonomy of arbuscular mycorrhizal fungi from phylum to species level. New Phytologist 193 970-984.

Kutschera, U. 2007. Plant-associated *Methylobacteria* as co-evolved photosymbionts. Plant Signaling and Behavior 2(2): 74-78.

Lane, D.J. 1991. 16S/23S rRNA sequencing. 115-178. *In* Stackerbrandt, E. and M. Goodfellow (eds.), *Nucleic acid techniques in bacterial systematics.* Wiley, New York.

Lehnert, M., M. Krug, and M. Kessler. 2017. A review of symbiotic fungal endophytes in lycophytes and ferns – a global phylogenetic and ecological perspective. Symbiosis 71:77–89.

Lodge, D.J., P.J. Fisher, B.C. Sutton. 1996. Endophytic fungi of *Manilkara bidentata* leaves in Puerto Rico. Mycologia 88: 733-38.

Muthukumar, T. and K. Prabha. 2013. Arbuscular mycorrhizal and septate endophyte fungal associations in lycophytes and ferns of south India. Symbiosis 59:15–33.

Naureen, Z., N.U. Rehman, H. Hussain, J. Hussain, S.A. Gilani, S.K.A. Housni, F. Mabood, A.L. Khan, S. Farooq, G. Abbas, A.A. Harrasi. Exploring the potentials for *Lysinibacillus sphaericus* ZA9 for plant growth promotion and biocontrol activities against phytopathogenic fungi. Frontiers in Microbiology 8.

Nelson, J. and A.J. Shaw. 2019. Exploring the natural microbiome of the model liverwort: fungal endophyte diversity in *Marchantia polymorpha* L. Symbiosis 75:45-59.

Niang, N., S. Demaneche, I. Ndoye, E. Navarro, and S. Fall. 2018. Genetic diversity of rhizobia and plant growth promoting rhizobacteria of soil under the influence of *Piliostigma reticulatum* (DC.) Hochst and their impact on shrub growth. African Journal of Agricultural Research 13(46): 2668-2679.

Oteino, N., R.D. Lally, S. Kiwanuka, A. Lloyd, D. Ryan, K.J. Germaine, and D.N. Dowling. 2015. Plant growth promotion induced by phosphate solubilizing endophytic *Pseudomonas* isolates. Frontiers in Microbiology 6: 745.

Pawlowska, J., M. Wilk, A. Sliwinska-Wyrzychowska, M. Metrak, and M. Wrzosek. 2014. The diversity of endophytic fungi in the above-ground tissue of two *Lycopodium* species in Poland. Symbiosis 63: 87-97.

Porras-Alfaro, A. and P. Bayman. 2011. Hidden fungi, emergent properties: endophytes and microbiomes. Annual Reviews in Phytopathology. 49:291-315.

PPG I. 2016. A community-derived classification for extant lycophytes and ferns. Journal of Systematics and Evolution 54:563-603.

Rognes, T., T. Flouri, B. Nichols, C. Quince, and F. Mahe. 2016. VSEARCH: a versatile open source tool for metagenomics. PeerJ 4: e2584.

Rajkumar, M, N. Ae, and H. Freitas. 2009. Endophytic bacteria and their potential to enhance heavy metal phytoextraction. Chemosphere 77: 153-160.

Rudgers, J.A., J.M. Koslow, and K. Clay. 2003. Endophytic fungi alter relationships between diversity and ecosystem properties. Ecology letters 7(1):42-51.

Saghai-Maroof, M.A., K.M. Soliman, R.A. Jorgensen, and R.W. Allard. 1984. Ribosomal DNA spacer-length polymorphisms in barley: Mendelian inheritance, chromosomal location, and population dynamics. PNAS 81:8014-8018.

Santi, C., D. Bogusz, and C. Franche. 2013. Biological nitrogen fixation in non-legume plants. Annals of Botany 111: 743-767.

Selosse, M-A., C. Strullu-Derrien, R. Martin, S. Kamoun, and P. Kenrick. 2015. Plants, fungi and oomycetes: a 400-million year affair that shapes the biosphere. New Phytologist 206:501-506.

Schmid, E. and F. Oberwinkler. 1993. Mycorrhiza-like interactions between the achlorophyllous gametophyte of *Lycopodium clavatum* L. and its fungal endophyte studied by light and electron microscopy. New Phytologist 124: 69-81.

Schulz, B., U. Wanke, and S. Draeger, H-J. Aust. 1993. Endophytes from herbaceous plants and shrubs: effectiveness of surface sterilization methods. Mycological research 97(12):1447-1450.

Shabanamol, S., K. Kivya, T.K. George, K.S. Rishad, T.S. Sreekumar, M.S. Jisha. 2018. Characterization and in planta nitrogen fixation of plant growth promoting endophytic diazotrophic *Lysinibacillus spharicus* isolated from rice (*Oryza sativa*). Physiological and Molecular Plant Pathology 102: 46-54.

Taylor, T. N. and M. Krings. 2005. Fossil microorganisms and land plants: associations and interactions. Symbiosis. 40:119–135.

Turner, S., K.M. Pryer, V.P.W. Miao, and J.D. Palmer. 1999. Investigating deep phylogenetic relationships among cyanobacteria and plastids by small subunit rRNA sequence analysis. Journal of Eukaryotic Microbiology 46:327-338.

Treu, R., G.A. Laursen, S.L. Stephenson, J.C. Landolt, and R. Densmore. 1996. Mycorrhizae from Denali National Park and Preserve, Alaska. Mycorrhiza 6:21–29.

U'Ren, J. M., F. Lutzoni, J. Miadlikowska, and A.E. Arnold. 2010. Community analysis reveals close affinities between endophytic and endolichenic fungi in mosses and lichens. Microbial Ecology 60:340–353.

Vilgalys R. and M. Hester. 1990. Rapid genetic identification and mapping of enzymatically amplified ribosomal DNA from several *Cryptococcus* species. Journal of Bacteriology 172(8):4238-4246.

Wang, Y., Z. Lai, X-X. Li, R-M.Yan, Z-B. Zhang, H-L. Yang, and D. Zhu. 2016. Isolation, diversity and acetylcholinesterase inhibitory activity of the culturable endophytic fungi harboured in *Huperzia serrata* from Jinggang Mountain, China. World Journal of Microbiology and Biotechnology 32.

Wilson, K. 2001. Preparation of genomic DNA from bacteria. Current Protocols in Molecular Biology. 56(1):2.4.1-2.4.5.

Winther, J. L. and W.E. Friedman. 2008. Arbuscular mycorrhizal associations in Lycopodiaceae. New Phytologist 177:790–801.

Zhao, Z. 2000. The arbuscular mycorrhizas of pteridophytes in Yunnan, southwest China: Evolutionary interpretations. Mycorrhiza 10:145–149.

Zhu, D, J. Wang, Q. Zeng, Z. Zhang, and R. Yan. 2010. A novel endophytic huperzine A-producing fungus, *Shiraia* sp. Slf14, isolated from *Huperzia serrata*. Journal of Applied Microbiology 109(4): 1469-1478.

Zubek, S., K. Piqtek, P. Naks, W. Heise, M. Wayda, and P. Mleczko. 2010. Fungal root endophyte colonization of fern and lycophyte species from the Celaque National Park in Honduras. American Fern Journal 100:126–136.

CHAPTER TWO

RE-EVALUATING THE SYSTEMATICS OF *DENDROLYCOPODIUM* USING RAD-SEQUENCING

2.1 Introduction

The taxonomy of what is now *Dendrolycopodium* (Lycopodiaceae) has long perplexed botanists. Fifty years after Linnaeus first described *Lycopodium obscurum* in 1753, Michaux described another species, *Lycopodium dendroideum* (Linnaeus, 1753; Michaux, 1803). Nearly ninety years later, D. C. Eaton reclassified *L. dendroideum* as a variety of *L. obscurum* (Eaton, 1890) and the debate over how to rank members of this group began. Fast forward to 1977, Hickey reexamined the *L. obscurum* complex and recognized three species: *L. dendroideum*; *L. juniperoideum*; and *L. obscurum* (including two varieties, var. *obscurum* and var. *isophyllum*) (Hickey, 1977, 1978). *L. obscurum* var. *isophyllum* was later elevated to species and named *L. hickeyi* (Wagner et al., 1989) and these four species were later split out of *Lycopodium* and distinguished as their own genus, *Dendrolycopodium* (Haines, 2003). Most recently, one more species, *D. verticale*, was recognized in China (Zhou and Zhang, 2017).

Unfortunately, this taxonomic story remains unresolved. Firstly, it is not known how *Dendrolycopodium* species are related to each other. Secondly, Lycopodiaceae is ranked sixth among the most hybridization-prone plant families (Whitney *et al*., 2010) and *Dendrolycopodium* is no exception to this trend. Hickey (1978) noted the existence of *Dendrolycopodium* plants which appeared to be of possible hybrid origin. These plants typically show an intermingling of supposedly

diagnostic traits, such as leaf ranking and angle of divergence from the main stem (Figure 2.1). This is consistent with mine and others' field observations (Haines, 2003; Weston Testo per. comm.). However, Hickey stated, "while it is impossible to prove the existence of hybrids in this species group, the secondary morphological evidence certainly suggests that hybridization does occur" (Hickey, 1978, pp. 48).

Finding evidence of hybrids is no longer such an impossible feat. Through the use of modern DNA sequencing technologies, we can now understand the population dynamics and evolutionary history of organisms better than ever before. However, such a study has not yet been conducted in *Dendrolycopodium* to elucidate potential hybrids and their origins (*i.e.* whether they are homoploid or polypoid hybrids). It has been suggested that hybrids in Huperzioideae and Lycopodielloideae (Figure 2.2) tend to be polyploid, but are predominantly homoploids in Lycopodioideae (Wagner *et al.,* 1985; Wagner, 1992). Phylogenetically based proclivities for homoploidy vs. polyploidy could provide insight into the reproductive mechanisms and genome structural elements that shape plant hybridization, speciation, and broad evolutionary trajectory. Here, I take the first step in this endeavor by conducting double-digest restriction-site associated sequencing (ddRAD-seq) on *Dendrolycopodium*.

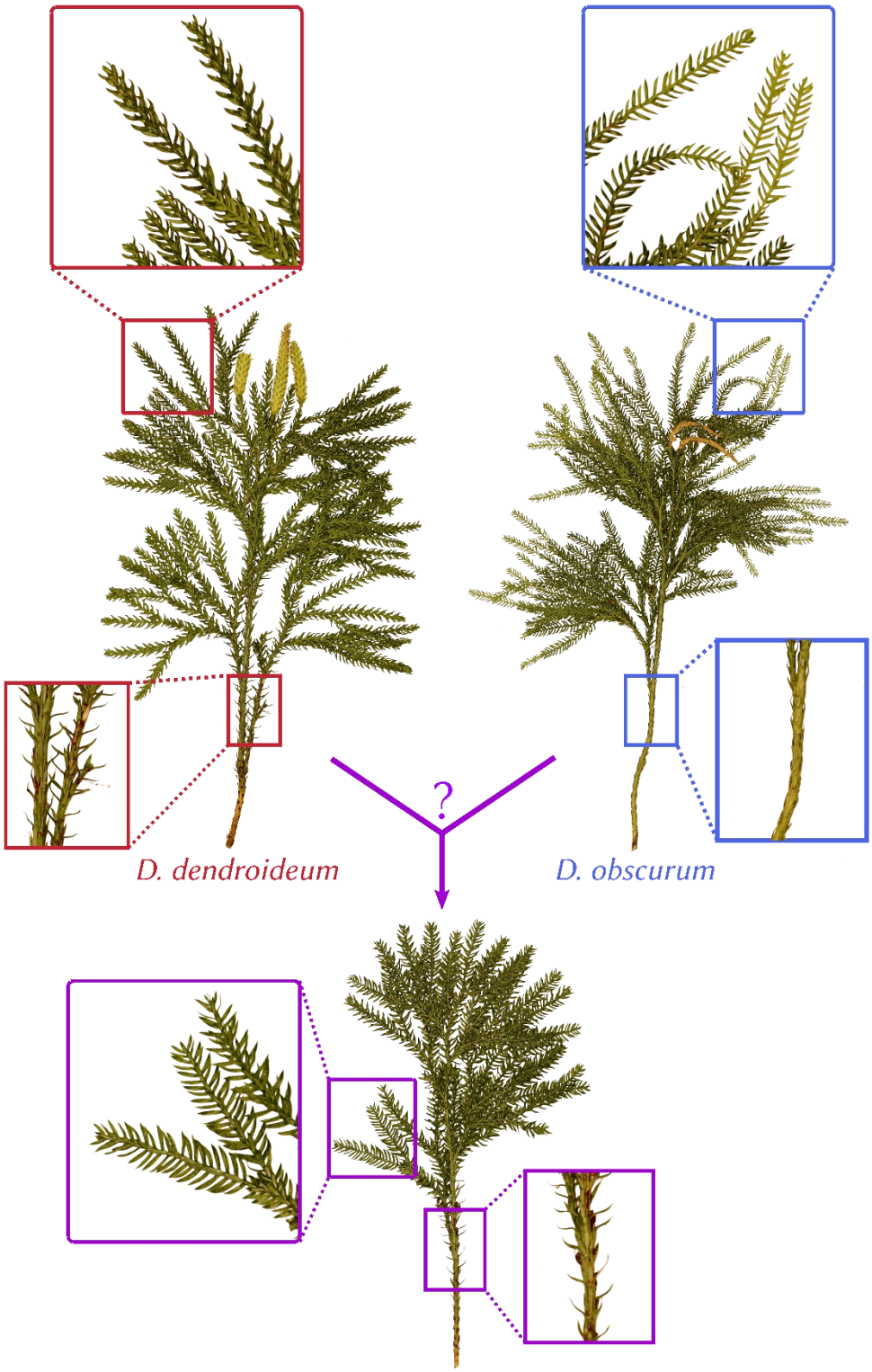

Figure 2.1 *Dendrolycopodium dendroideum, D. obscurum*, and hybrid (ARP0012) showing intermingling diagnostic characters (leaf arrangement and divergence angle) collected from McLean Bogs in NY (42.54795, -76.26633)

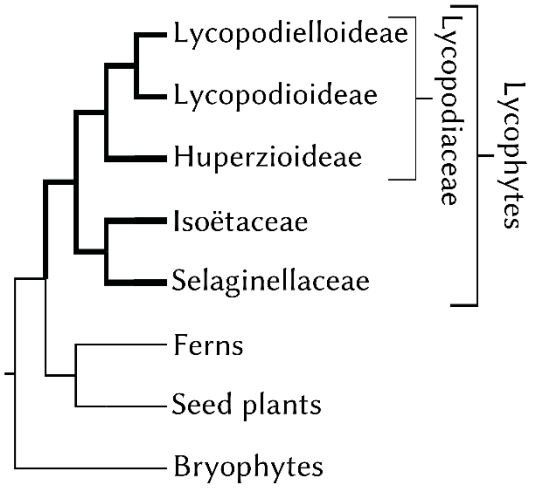

Figure 2.2 Phylogeny of Lycopodiaceae subfamilies (PPG I, 2016)

2.2 Methods

2.2.1 Collections

Fresh materials were collected from central New York. A few branches were silica dried for DNA extractions. To achieve the best geographic coverage, herbarium specimens and silica-dried material collected after 1995 were also sampled (Figure 2.3; Appendix 7). Samples which did not clearly key to a species or showed intermediate morphology were called *Dendrolycopodium sp.* (*D. sp.*).

2.2.2 DNA extractions & library preparation

Dried tissue samples (0.01-0.03g) were added to a 2mL tube with two, 3.5mm stainless steel balls. Tubes were then submerged in liquid nitrogen and shaken at 1500 strokes per minute on a MiniG 1600 (SPEX Sample Prep). DNA extractions were completed using a modified CTAB protocol (Saghai-Maroof *et al*., 1984; Appendix 1). Extraction concentrations were quantified using the HS Qubit

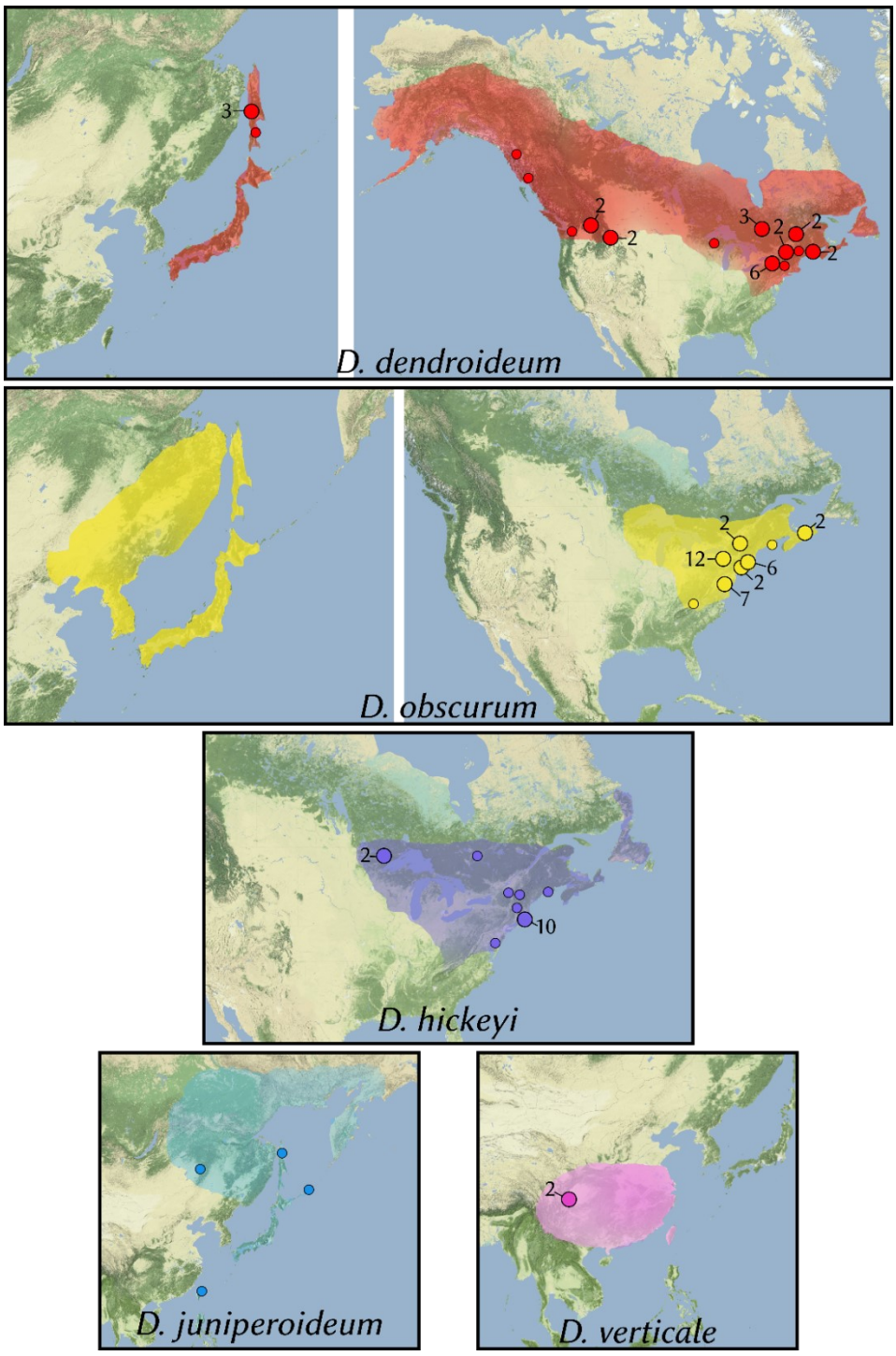

Figure 2.3 Geographic distribution of samples: points represent samples used in this study; numbers correspond to the number of samples from that area, unlabeled points represent one sample; estimated ranges are highlighted. Not pictured: 10 unidentifiable *Dendrolycopodium sp.* from Central NY, USA and 1 from Sakhalin Island, Russia. Maps made in QGIS (v. 3.10.2) using background maps by Stamen Design, edited in Adobe Photoshop Elements (15.0) and Inkscape (0.92.3).

Kit (Invitrogen). A double-digest RAD-sequencing protocol was chosen over single-digest, despite the increased likelihood for locus dropout, because single-digest would have been prohibitive given the relatively large *Dendrolycopodium* genome size. Libraries were prepared based on a protocol by Parchman *et al.* (2012), with modifications by Nicolas Devos and Duncan Hauser. Samples were digested using EcoRI and MseI restriction enzymes, ligated to barcoded adaptors, and amplified (Figure 2.4, see Appendix 8, 9 for protocol details). The HS Qubit kit (Invitrogen) was used to quantify sample recovery after PCR. 50ng from each sample were then pooled and SparQ beads (Quanta Bio) were used for a 250-500bp size selection. The resultant library was submitted to Cornell's Genomics Facility and sequenced on Illumina NextSeq 500 (150bp single-end, high output flowcell).

Figure 2.4 Sequencing construct design

2.2.3 Data processing

Raw sequence files were processed using Cutadapt (v. 1.18, Martin, 2011) to remove poly-G tails resulting from 2-color Illumina chemistry, Illumina adapters, and poly-A tails as well as demultiplex (allowing up to one mismatch in each barcode; commands: cutadapt –nextseq-trim=20; cutadapt -a "A{100}" –minimum length 60; cutadapt -e 0.15 –no-inels -g file:barcodes). Trimmed, demultiplexed sequences were then processed using iPyrad (v. 0.7.30, Eaton, 2014). For the full data set, cleaned reads were mapped to a *Dendrolycopodium obscurum* draft genome

(Table 2.1) and unmapped reads were clustered *de novo.* Reads were clustered at 88% identity with a minimum depth of 6 reads within individual samples, a maximum depth of 10,000 reads within samples, and a minimum cluster depth of 4 samples between individual samples. Poorly performing samples (<1000 loci) were removed after processing in iPyrad.

Table 2.1 *D. obscurum* draft genome statistics (JGI)

Sequencing platform	NovaSeq
Estimated genome size	4.79Gb
Assembled genome size	4.55Gb
% Repeats	40%
% Contamination	2%
Scaffold number	3,484,908
Scaffold n50	4.3kb
Contig number	4,321,281
Contig n50	2.8 kb
Scaffold contig coverage	97.97%
% gap	2%

2.2.4 Phylogenetic tree

Maximum likelihood phylogenies were inferred for the SNPs data output (from iPyrad) using RAxML-HPC v.8.2.12 on XSEDE (Stamatakis, 2014) with a general time reversible model of nucleotide substitution drawing rates from the CAT approximation of rate heterogeneity (GTRCAT). To search for the best tree, 50 independent runs with different starting points were executed. Branch supports were

assessed with 500 non-parametric bootstrap replicates. Tree files were processed in FigTree (Rambaut, 2012) and exported as SVG files for formatting in Inkscape (0.92.3).

2.2.5 STRUCTURE analyses

STRUCTURE files were created by iPyrad and analyzed in STRUCTURE (v. 02.3.4, Pritchard *et al.,* 2000). Because STRUCTURE is sensitive to missing data, input files were created containing only loci shared by at least 20 samples. Five data sets were used for STRUCTURE analyses: one containing all *Dendrolycopodium* samples, and four data sets for hierarchical analyses (Janes *et al.,* 2017) of each of the major clades detected in the initial STRUCTURE output. All STRUCTURE analyses were run for 100,000 Markov chain Monte Carlo (MCMC) generations (50,000 burn-in and 50,000 analysis generations), under default parameters with admixture for K=2 to K=5 with 3 replicates at each K-value. Outputs were viewed using STRUCTURE HARVESTER (Earl and von Holdt, 2012). Optimal K values were assessed by selecting the value for which the slope of the natural log probability was highest (Evanno *et al.,* 2005). STRUCTURE plots were created using STRUCTURE PLOT (v. 2.0, Ramasamy *et al.,* 2014).

2.3 Results

Sequencing yielded around 563 million reads from 102 samples. After cleaning and demultiplexing, around 470 million reads remained. After processing in iPyrad, 13 poor performing samples were removed, resulting in the following samples counts per species: 2 *D. verticale;* 5 *D. juniperoideum*; 28 *D. obscurum;* 14

D. hickeyi; 20 *D. dendroideum*; and 11 *D. sp.* samples that were not clearly identifiable.

2.3.1 Phylogenetic tree

The maximum likelihood phylogeny supports four major clades, which are reflected in the STRUCTURE data. The *D. obscurum* clade is the earliest diverging and is supported with a bootstrap value of 100. With a bootstrap value of only 57, the *D. hickeyi* clade is not as well supported. *D. hickeyi* samples are split into two smaller, well supported clades (BS=100) which are not mirrored in the hierarchical STRUCTURE subgroupings. The split between *D. dendroideum* and the Asian samples is well supported. Within the Asian samples, *D. juniperoideum* is not recovered as monophyletic.

2.3.2 STRUCTURE analyses

The STRUCTURE analysis had an optimum at K=3. However, there was little difference in the likelihood values between K=3 and K=4. The K=3 result fails to separate the Asian samples as a distinct group, likely due to the limited sampling in the area. Because K=4 distinguishes this clade, which is evident in the phylogeny, it reflects a more accurate grouping (Figure 2.7). The first group consists entirely of *D. dendroideum* samples ("*D. denroideum* group"). The second ("*D. obscurum* group") includes mostly *D. obscurum*, except for two *D. hickeyi* samples and one *D. sp.* The third group ("*D. hickeyi* group") includes 9 *D. sp.* samples and the remaining *D. hickeyi* samples. The fourth group encompassed all of the Asian samples including *D. verticale*, *D. juniperoideum*, *D. dendroideum,* and *D. sp.* (the

"Asian group"). Three hybrids were detected between the *D. dendroideum* and *D. obscurum* groups and one between the *D. dendroideum* and Asian groups.

Hierarchical STRUCTURE analyses for each of the four clades detected subdivisions. In the *D. dendroideum* group, three subgroups were detected, with no admixture detected between them. In the *D. obscurum* group, four subgroups were detected, with some admixture. In the *D. hickeyi* group, three subgroups were detected with some clearly admixed samples. In the Asian group, three subgroups were detected, with one sample a clear mix between the second and third subgroup.

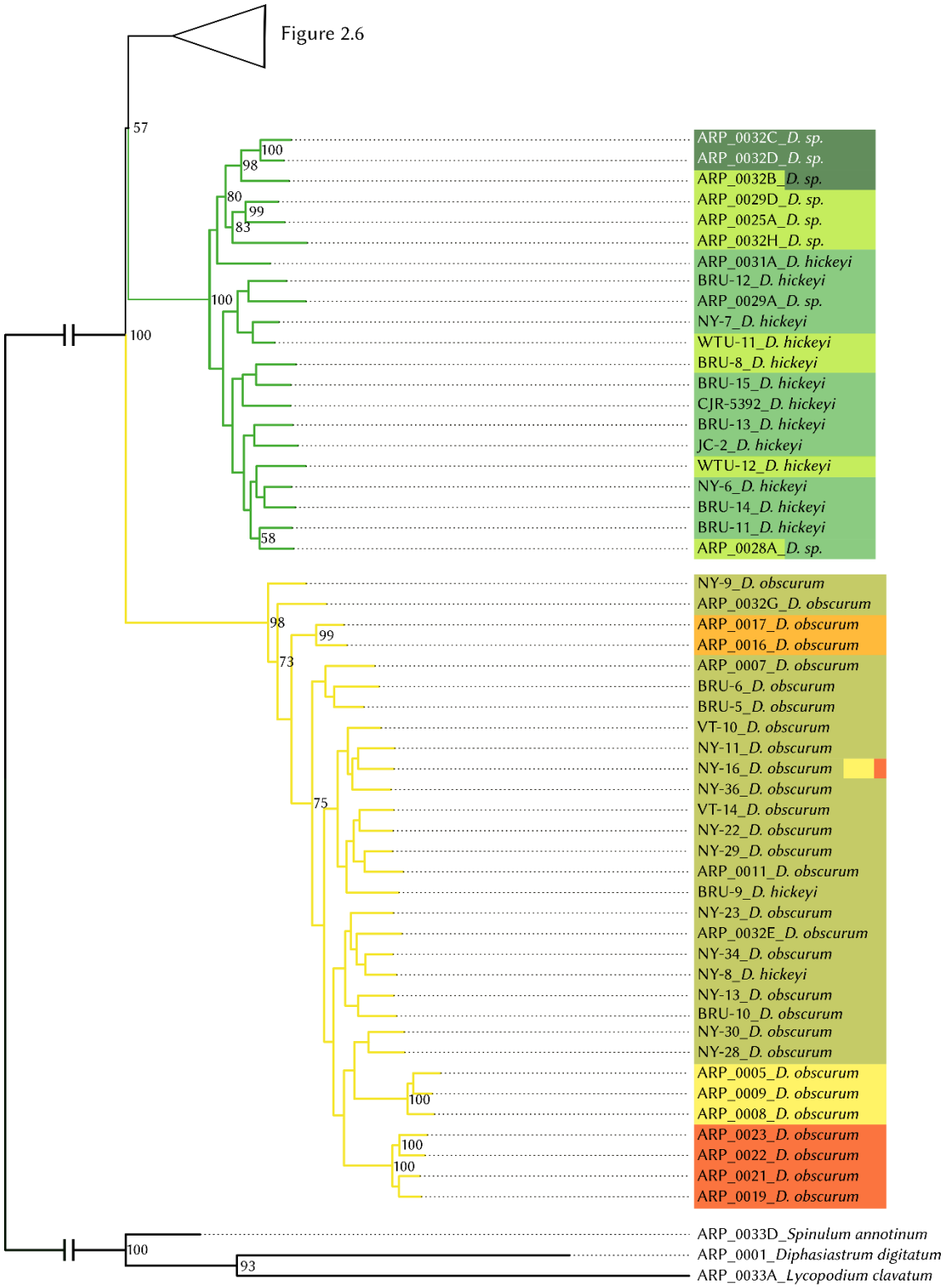

Figure 2.5 RAxML phylogenetic tree: best tree produced from 50 alternate starting runs (likelihood= -2703881.2); node labels represent bootstrap values (values <50 not pictured). Colors correspond to STRUCTURE groupings (Figure 2.7).

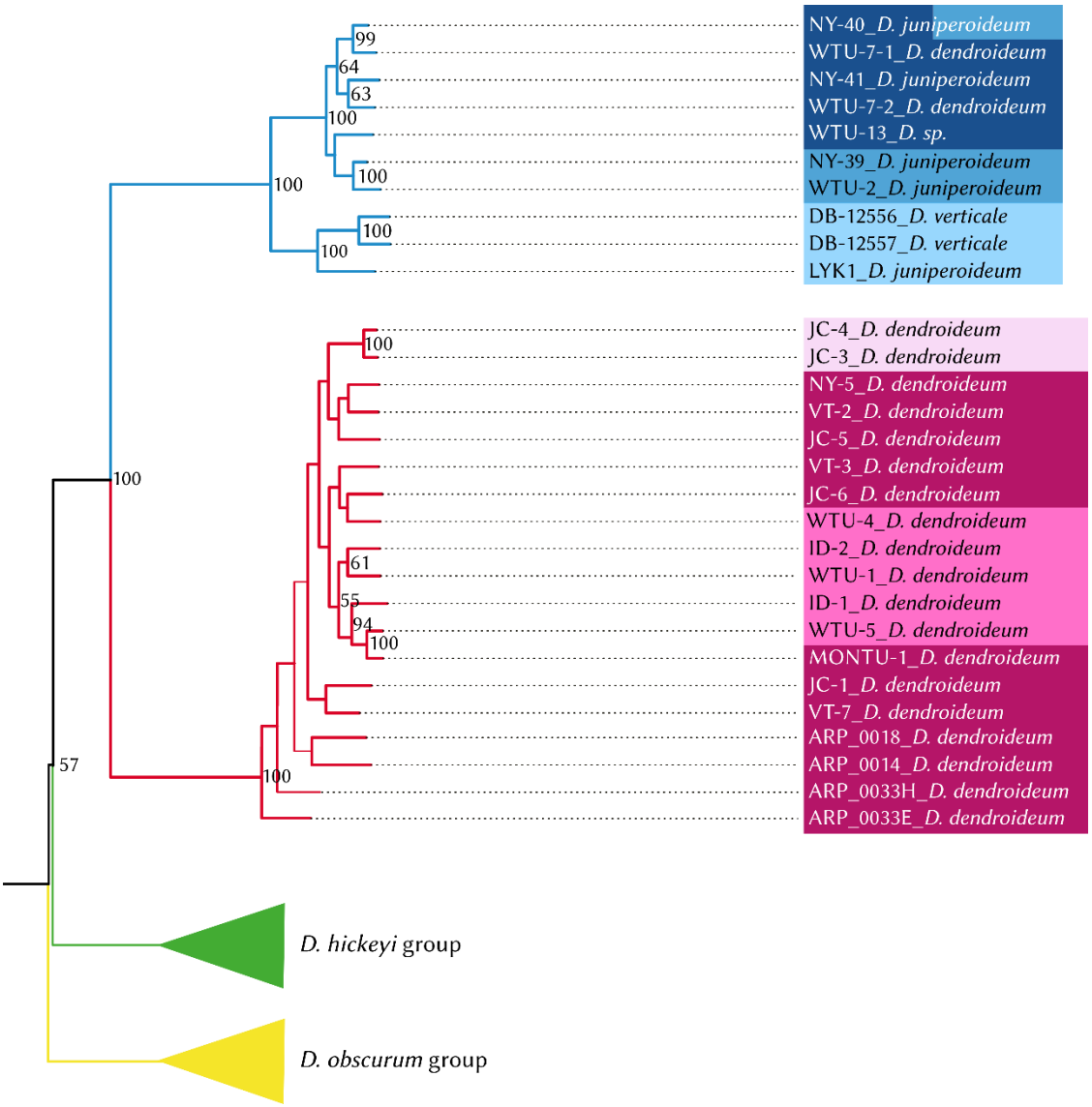

Figure 2.6 RAxML phylogenetic tree, continued: best tree produced from 50 alternate starting runs (likelihood= -2703881.2); node labels represent bootstrap values (values <50 not pictured). Colors correspond to STRUCTURE groupings (Figure 2.7).

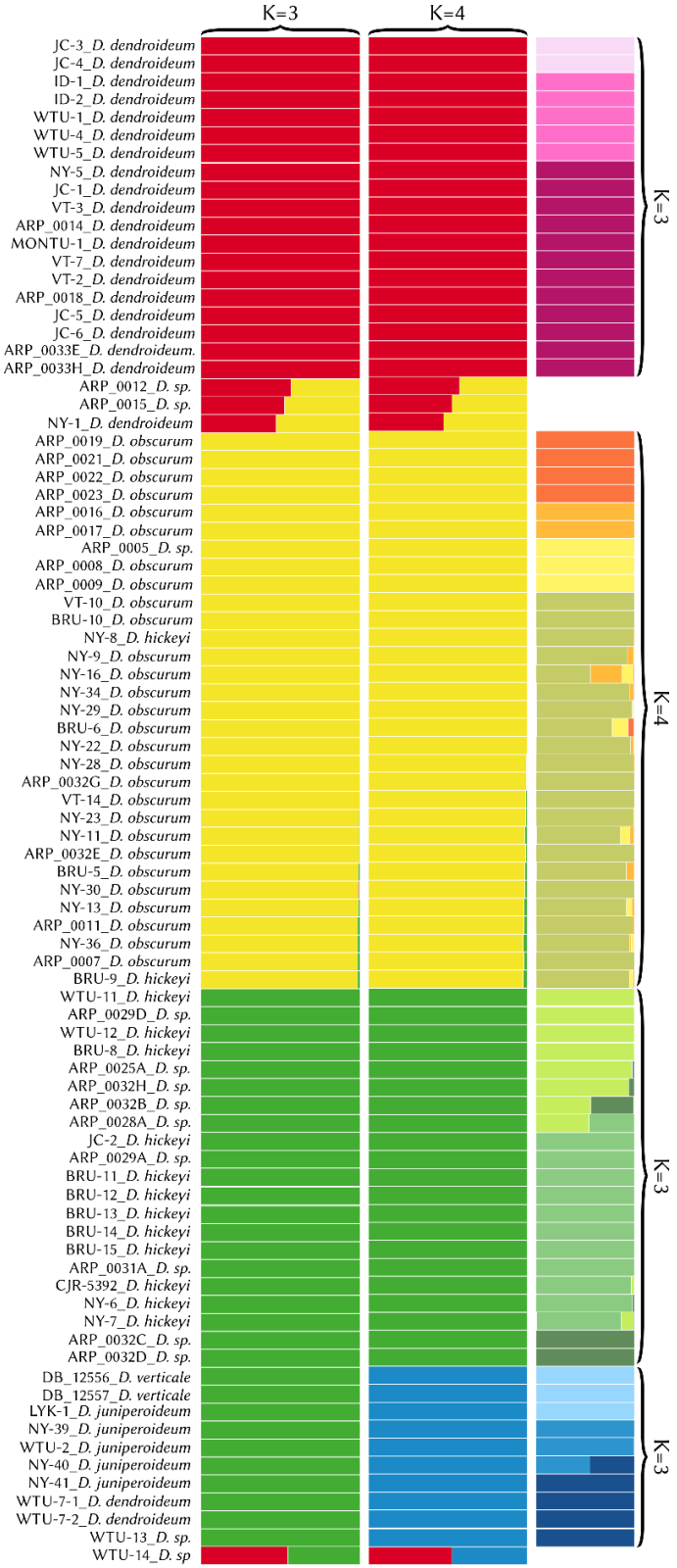

Figure 2.7: STRUCTURE results (K=3 vs. K=4), with the hierarchical results in the far right column. Detailed sample information can be found in Appendix 7.

2.4 Discussion

Overall, both the phylogeny and the STRUCTURE results indicate that *D. dendroideum, D. obscurum,* and *D. hickeyi* represent distinct genetic entities. Furthermore, as it currently stands, the morphotaxonomy is a somewhat reasonable reflection of phylogenetic history, however it is insufficient on its own. Both NY-8 and BRU-9 key very clearly to *D. hickeyi*, yet they fall into the *D. obscurum* clade (Figure 2.5, 2.7). Additionally, many samples in the *D. hickeyi* clade cannot clearly be identified as such from the current species descriptions and keys; some even show an intermingling of traits specific to other species despite not being recovered as hybrids.

Phylogenetic and STRUCTURE results also indicate that all the Asian samples included in this study represent a separate distinct genetic entity comprised of a few described species: *D. verticale*, *D. juniperoideum*, and *D. dendroideum*. Despite being clearly morphologically different from the other described taxa, *D. juniperoideum* is not recovered as monophyletic. Further sampling and a thorough review of morphology should be conducted to evaluate the validity of *D. juniperoideum*. Additionally, samples identified as *D. dendroideum* in this clade appear to be a separate genetic entity from those in the main *D. dendroideum* group. Again, more sampling and a detailed morphological review of the *D. dendroideum* in Asia is required to determine the taxonomic fate of these plants.

2.4.1 Hybrids

Four interspecific hybrids were identified from STRUCTURE analyses. All *D. dendroideum x obscurum* samples (ARP_0012, ARP_0015, and NY-1) have a

chimeric appearance, with some parts of the plant matching the characters of *D. dendroideum* and others matching *D. obscurum* (see Figure 2.1). WTU-14 (*D. denroideum x* Asia clade), however, simply resembles *D. dendroideum*. From this data, it is impossible to determine if any of these hybrids are polyploid.

2.4.2 Hierarchical STRUCTURE results and geography

Many of the finer groupings resulting from the hierarchical STRUCTURE analysis are reflected in their distribution. Within the *D. dendroideum* group, ID-1, ID-2, WTU-1, WTU-4, and WTU-5 are all from western North America. (Figure 2.8). MONTU-1 is also from western North America, but is more genetically similar to the remainder of the samples from the East.

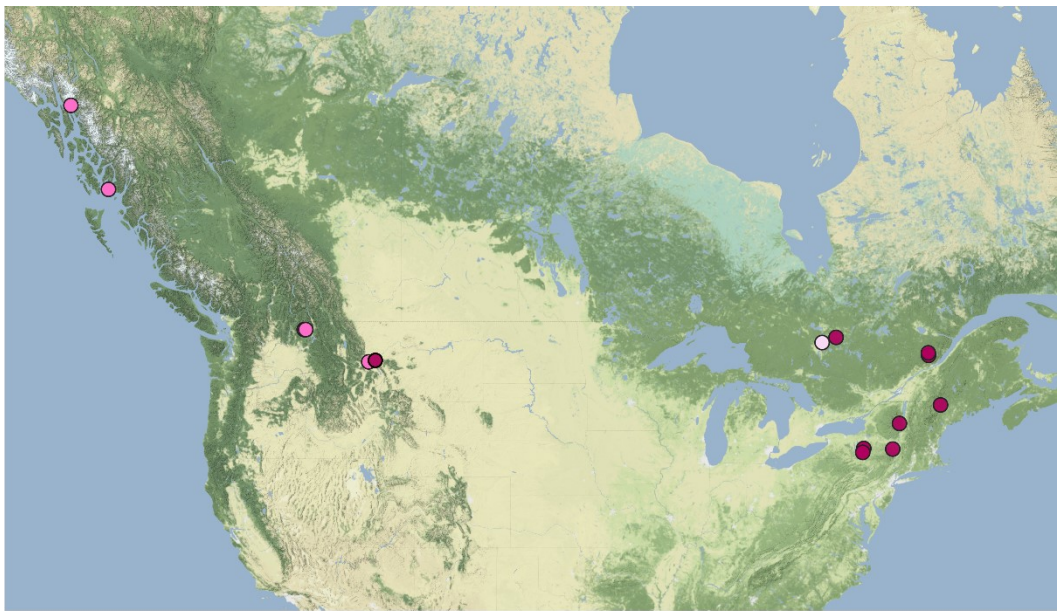

Figure 2.8 *D. dendroideum* group distribution; colors correspond to the hierarchical STRUCTURE results in Figure 2.7. Map created in QGIS (v. 3.10.2) using background map by Stamen Design

Within the *D. obscurum* group, all four genetic sub-entities discovered in the hierarchical STRUCTURE analysis occur in McLean Bogs, New York (42.54795, -76.26633), with three of the four sub-entities only being found there (Figure 2.9). It is possible that this area acted as a refuge during glaciation, thus more ancient genetic diversity was preserved here. A detailed sampling of *D. obscurum,* with more evenly distributed coverage of its range, would be required to determine if these genetic sub-entities occur elsewhere or if there are more pockets of hidden genetic diversity of *D. obscurum.*

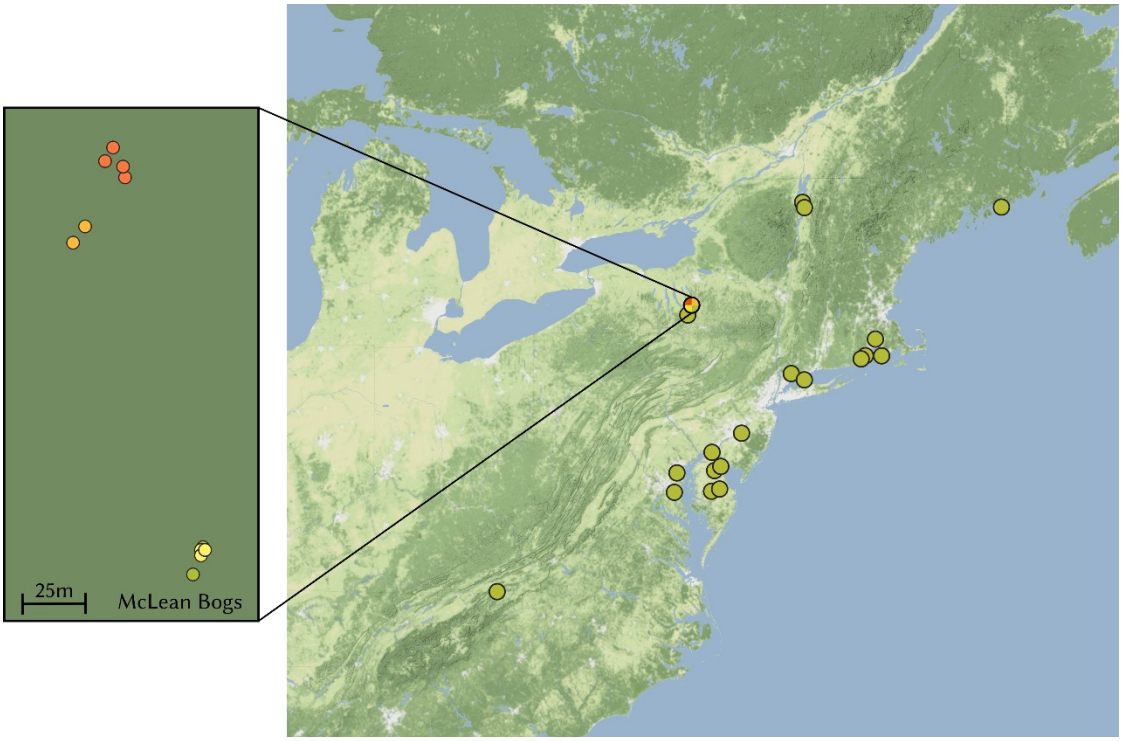

Figure 2.9 *D. obscurum* group distribution; colors correspond to the hierarchical STRUCTURE results in Figure 2.7. Map created in QGIS (v. 3.10.2) using background map by Stamen Design, edited in Inkscape (v. 0.92.3)

Within the *D. hickeyi* group, there does not appear to be a relationship between geographic distribution and the genetic sub-entities described by the

hierarchical STRUCTURE analysis (Figure 2.10). All genetic sub-entities occur in central NY, where around nearly half of the *D. hickeyi* group samples were collected.

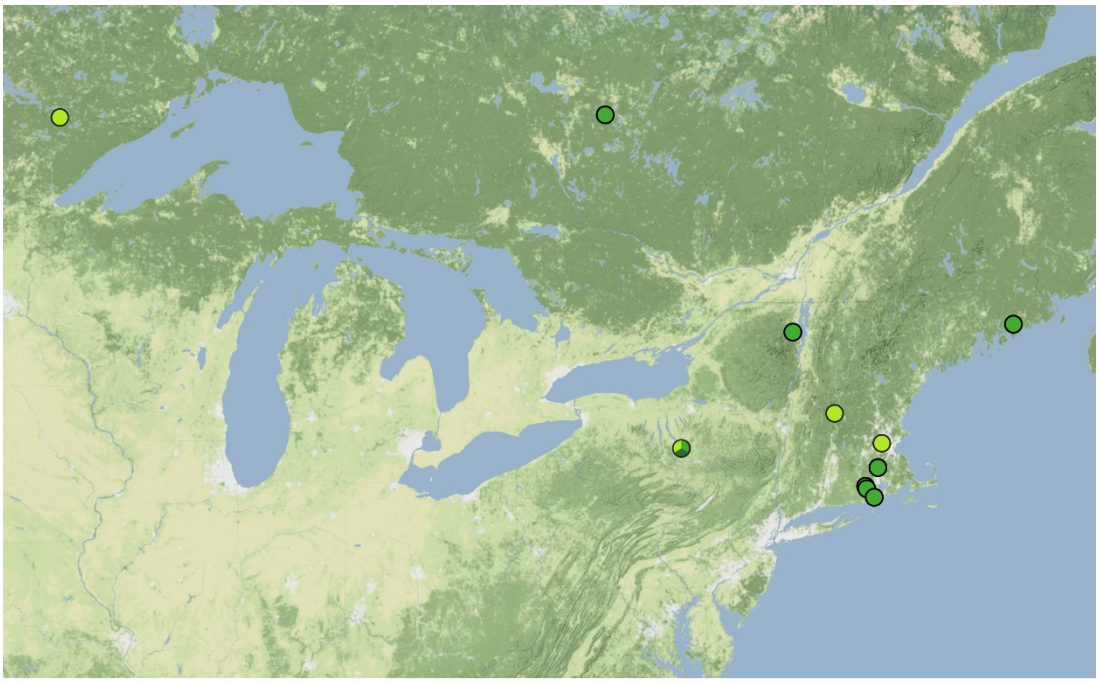

Figure 2.10 *D. hickeyi* group distribution; colors correspond to the hierarchical STRUCTURE results in Figure 2.7. Map created in QGIS (v. 3.10.2) using background map by Stamen Design, edited in Inkscape (v. 0.92.3)

Finally, the samples within the Asian clade split into two distinct geographic groupings with DB-12556, DB-12557, and LYK-1 in the more southern group and NY-39, NY-40, NY-41, WTU-7-1, WTU-7-2, and WTU-13 located further north (Figure 2.11). As stated previously, *D. juniperoideum* does not appear to be monophyletic and is represented in both of these groups. Once again, thorough sampling throughout the range of *Dendrolycopodium* in Asia is crucial to elucidating the genetic diversity of this region and reevaluating the taxonomy.

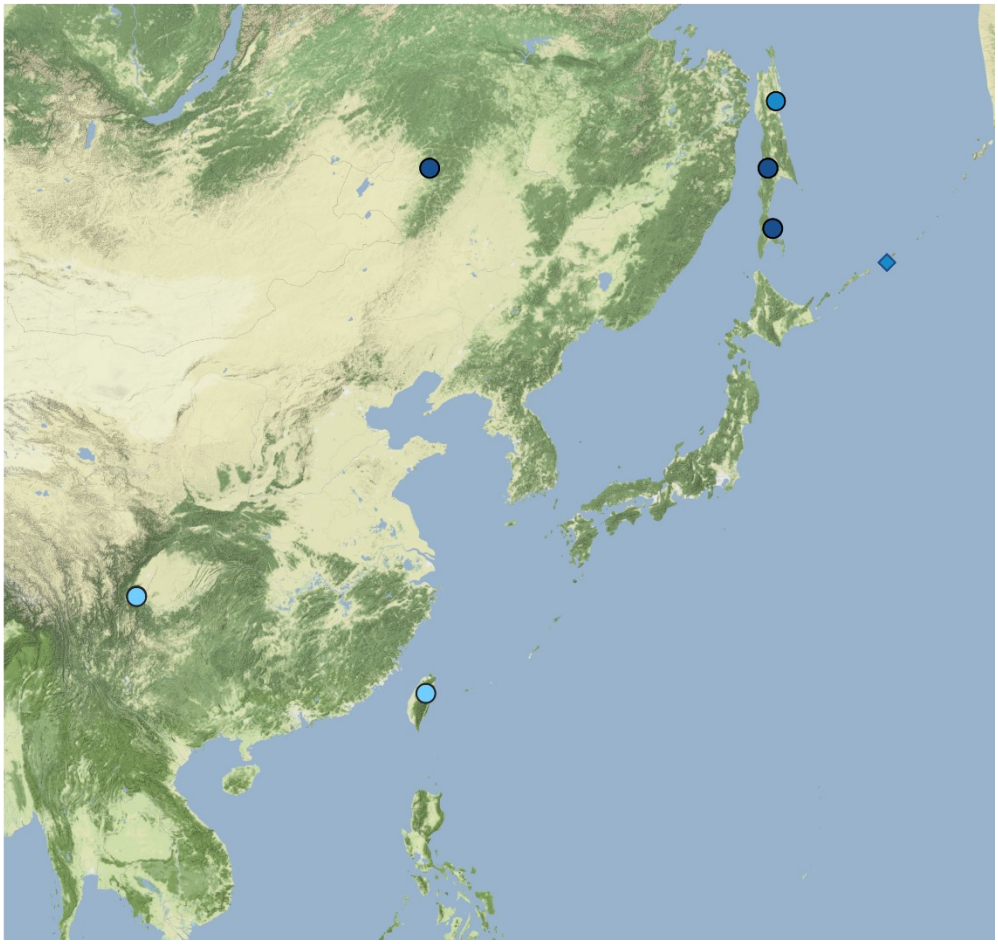

Figure 2.11 Asian group distribution; colors correspond to the hierarchical STRUCTURE results in Figure 2.7. The diamond represents NY-40, which appears to be a hybrid between the two northern sub-entities. Map created in QGIS (v. 3.10.2) using background map by Stamen Design

2.4.3 Taxonomic recommendations

The North American *D. obscurum, D. dendroideum,* and *D. hickeyi* are supported as monophyletic by the genetic data and thus should remain valid taxa. Morphometric analyses should be revisited to reliably distinguish them from one another and their hybrids. However, the taxonomy of the Asian *Dendrolycopodium* must be revised as *D. juniperoideum* is not supported as monophyletic and the Asian *D. dendroideum* does not clade with the bulk of *D. dendroideum.* As such, I

tentatively recommend that all members of this clade be renamed *D. juniperoideum* as it predates the name *D. verticale.* I recognize that this creates a group that cannot be defined with even the clearest of morphological characters (*e.g.* number of leaves per rank differs between *D. juniperoideum and D. verticale*) and must instead rely on geography. I suspect that further sampling may warrant the distinction of species between the northern (*i.e.* Russia, Japan, Korea) and southern (*i.e.* China, Taiwan) extent of the range, in which case, the name *D. verticale* should be resurrected for the southern group. However, the data presented here lack the sampling, as well as morphological features, to support this. I cannot stress enough the need for further study and revision of the taxonomy of *Dendrolycopodium* in Asia.

REFERENCES

Earl, D.A. and B.M. vonHoldt. 2012. STRUCTURE HARVESTER: a website and program for visualizing STRUCTURE output and implementing the Evannop method. Conservation Genetics Resources, 4: 359-361.

Eaton, D.A.R. 2014. PyRAD: Assembly of *de novo* RADseq loci for phylogenetic analyses. Bioinformatics 30:1844-1849.

Eaton, D.C. 1890. Ferns and fern allies. Pp. 675--701, *In* A. Gray (ed.), *Gray's manual of botany of the northern United States*. American Book Company, New York.

Evanno, G., S. Regnaut, and J. Goudet. 2005. Detecting the number of clusters of individuals using the software STRUCTURE: a simulation study. Molecular Ecology 14: 2611-2620.

Haines, A. 2003. *The families Huperziaceae and Lycopodiaceae of New England.* V.F. Thomas Company.

Hickey, R.J. 1977. The *Lycopodium obscurum* complex in North America. American Fern Journal 67(2):45-48.

Hickey, R.J. 1978. Variability in the *Lycopodium obscurum* complex of North America and eastern Asia. MS thesis, Miami University.

Janes, J.K., J.M. Miller, J.R. Dupuis, R.M. Malenfant, J.C. Gorell, C.I. Cullingham, and R.L. Andrew. 2017. The K=2 conundrum. Molecular Ecology 26: 3594-3602.

Linnaeus, C. 1753. *Species plantarum.* pp. 1102-1103.

Martin, M. 2011. Cutadapt removes adapter sequences from high-throughput sequencing reads. EMBnet. Journal 17(1):10-12.

Michaux, A. 1803. *Flora boreali-americana.* Pp 282.

Parchman, T.L., Z. Gompert, J. Mudge, F.D. Schilkey, C.S. Benkman, and C.A. Buerkle. Genome-wide association genetics of an adaptive trait in lodgepole pine. Molecular Ecology 21:2991-3005.

PPG I. 2016. A community-derived classification for extant lycophytes and ferns. Journal of Systematics and Evolution 54:563-603.

Pritchard, J.K., M. Stephens, and P. Donnelly. 2000. Inference of population structure using multilocus genotype data. Genetics 155:945-959.

Ramasamy, R.K., S. Ramasamy, B.B. Bindroo, and V.G. Naik. 2014. STRUCTURE PLOT: a program for drawing elegant STRUCTURE bar plots in user friendly interface. Springer Plus 3: 431.

Rambaut, A. 2012. FigTree v. 1.4. Molecular evolution, phylogenetics and epidemiology. University of Edinburgh, Institute of Evolutionary Biology, Edinburgh, UK.

Saghai-Maroof, M.A., K.M. Soliman, R.A. Jorgensen, and R.W. Allard. 1984. Ribosomal DNA spacer-length polymorphisms in barley: Mendelian inheritance, chromosomal location, and population dynamics. PNAS 81:8014-8018.

Stamatakis, A. 2014. RaxML version 8: a tool for phylogenetic analysis and post-analysis of large phylogenies. Bioinformatics 30: 1312-1313.

Wagner, F.S. 1992. Cytological problems in *Lycopodium s.l.* Annals of the Missouri Botanical Garden 79:718-729.

Wagner, W.H., F.S. Wagner, and J.M. Beitel. 1985. Evidence for interspecific hybrids in pteridophytes with subterranean mycoparasitic gametophytes. Proceedings of the Royal Society of Edinburgh 86B:273-281.

Wagner, W.H., J.M. Beitel, and R.C. Moran. 1989. *Lycopodium hickeyii*: a new species of North American clubmoss. American Fern Journal 79:119-121.

Whitney, K.D., J.R. Ahern, L.G. Campbell, L.P. Albery, and M.S. King. 2010. Patterns of hybridization in plants. Perspectives in Plant Ecology, Evolution, and Systematics 12:175-182.

Zhou, X-M., and L-B. Zhang. 2017. *Dendrolycopodium verticale* comb. nov. (Lycopodiopsida: Lycopodicaeae) from China. Phytotaxa 295(2):199-200.

CHAPTER THREE

FERNS: THE FINAL FROND-TIER IN PLANT MODEL SYSTEMS

3.1 Introduction

With over 12,000 species (PPG I, 2016), ferns are a diverse lineage that is integral to understanding terrestrial plant evolution and ecology. For example: How has the diversity of life cycles evolved? What genetic, molecular, and ecological mechanisms have governed major life cycle changes? What mechanisms control the tracheophyte body plan and how have they evolved through time?

The alternation of generations (phases) life cycle is common to all embryophytes. However, the life cycle of ferns and lycophytes is unique because the sporophyte and gametophyte generations are independent, and the sporophyte is generally considered the dominant phase (although gametophytes of certain species can be long-lived, e.g., *Vittaria appalachiana* Farrar & Mickel (Farrar, 1967)). This contrasts with bryophytes, which produce a sporophyte that is dependent on the dominant gametophyte, and seed plants in which gametophytes are highly reduced, encased within, and completely dependent on the dominant sporophyte. The transition between the haploid-dominant and sporophyte-dominant life cycle likely had a profound impact on plant evolution (Gerrienne and Gonez, 2011; Haufler *et al*., 2016; Qiu, Taylor and McManus, 2012). Ferns are therefore an ideal system to study the mechanisms that determine sporophyte and gametophyte development in comparison to other land plants. Land plant life cycles also vary in the types of spores they produce and the sexual condition of the gametophytes. For example, the Salviniales, Selaginellales, Isoëtales, and all seed plants are heterosporous, meaning

the sporophyte produces megaspores (in megasporangia) and microspores (in microsporangia). These spores germinate and become gametophytes that are endosporic (i.e., they develop within the spore wall) and dioicous. The vast majority of ferns, on the other hand, are exosporic and homosporous, meaning the sporophyte produces spores that are all the same size and that have the potential to develop into monoicous gametophytes. *Platyzoma microphyllum* R.Br. (Pteridaceae) is a curious outlier to these two general life cycle formats—it is heterosporous, but exosporic and can produce monoicous gametophytes (Tryon and Vida, 1967; Duckett and Pang, 2014). The transition between homospory and heterospory has occurred independently many times across land plant evolution. Ferns are an excellent system to provide insight into the mechanisms that govern this transition by comparing the biology of the homosporous ferns to the heterosporous ferns (Salviniales) and the seed plants. Furthermore, across vascular plants, homospory is correlated with a higher chromosome numbers and larger genome sizes compared to heterospory. While the reason for this correlation is not fully understood (Wolf *et al.*, 2015), it has been hypothesized that high levels of polyploidy could maintain genetic diversity in organisms with a high potential for inbreeding, linked with the production of monoicous gametophytes (Klekowski and Baker, 1966; but see Haufler and Soltis, 1986). Indeed, homosporous ferns have notoriously large genomes (average=13.82 Gb, range=1.95 - 73.19 Gb; Kuo and Li, 2019) and represent one of the final frontiers in exploring plant genome space.

Ferns are also pivotal in studying the evolutionary development of vascular plant body plans. Stem-leaf-root anatomy has evolved in the sporophyte multiple

times throughout the history of land plants (Boyce, 2005; Hetherington and Dolan, 2018). To truly understand the mechanisms that govern the evolution of this anatomy, comparative genetic studies need to compare multiple lineages of land plants. For example, by focusing on a lycophyte *Selaginella kraussiana* (Kunze) A. Braun and a fern *Osmunda regalis* L., Harrison *et al.* (2005) were able to show that the same genetic pathway (in this case KNOX-ARP interaction) was independently recruited for the convergent evolution of leaves. Similar comparative studies in the future will provide not only new insights into the field of plant evo-devo, but will also reveal the genetic mechanisms that may have developed uniquely in ferns.

Although ferns are essential to understanding land plant evolution through comparisons with other lineages, they are also interesting in their own right. The sex of many homosporous ferns can be influenced by their environment, a phenomenon unknown in other plant lineages. For example, the gametophytes of proposed model *Ceratopteris richardii* may be either male or hermaphroditic. Hermaphroditic gametophytes secrete a compound called antheridiogen, which promotes development of neighboring gametophytes as exclusively antheridial (Eberle *et al.*, 1995). Other biotic and abiotic factors, such as light (Kamachi *et al*., 2007) and soil bacteria (Ganger *et al.*, 2019), can also influence gametophyte sex expression. In addition, no other plants are known to engage in a vertically transmitted cyanobacterial symbiosis like *Azolla* (Wagner, 1997), making *Azolla* an excellent system to study symbiosis biology. Finally, few plants can accumulate arsenic levels as high as *Pteris vittata* L. (Ma *et al*., 2001), making it an ideal system for studying the cellular and molecular mechanisms involved in heavy metal tolerance.

Despite their utility for studying plant evolution, development, molecular biology, and ecology, a model fern has not yet been completely developed. A fully functional model requires a high-quality reference genome and efficient transformation methods. Additionally, they should not be polyploid, should be easily maintained in a laboratory environment, and have a relatively short generation time. Among ferns, only the genomes of *Azolla filiculoides* Lam. and *Salvinia cucullata* Roxb. have been sequenced (Li *et al.,* 2018), but genetic manipulation tools are lacking in these species (Table 3.1). On the other hand, transformation techniques have been developed for species that lack a fully sequenced genome, including: *Marsilea vestita* Hook. & Grev., *Adiantum capillus-veneris* L., *Pteris vittata*, and *Ceratopteris richardii* Brongn. (Table 3.1; Bui *et al*., 2015; Kawai *et al*., 2003; Kawai-Tooyooka *et al.*, 2004; Klink and Wolniak, 2000; Muthukumar *et al.*, 2013; Plackett *et al*., 2014, 2015; Stout *et al*., 2003). In this review, we describe potential model ferns, as well as the tools and resources that have already been developed for each.

3.2 Azolla filiculoides & Salvinia cucullata

Azolla and *Salvinia* are genera of floating aquatic ferns belonging to the Salviniacaeae. This family and its sister lineage Marsileaceae, are the only heterosporous ferns (Figure 3.1; PPG 1, 2016). The relationships of species within the genus *Azolla* require further resolution, but it likely contains five to seven species (Evrard and Van Hove, 2004; Metzgar, Schneider, and Pryer, 2007; Reid, Plunkett, and Peters, 2006). *Salvinia* consists of around twelve species, and the position of *S. cucullata*, in particular, is uncertain (Nagalingum, Schneider and Pryer, 2008).

Table 3.1. Summary of characteristics and available tools for each prospective model

Species	Family	Ploidy	Homosporous/ heterosporous	Genome	Transformation methods				
					RNAi	DNAi	*Agrobacterium*-mediated	Particle bombartment	CRISPR/Cas9
Azolla filiculoides	Salviniaceae	Diploid	Heterosporous	Li et al. 2018	-	-	-	-	-
Salvinia cucullata	Salviniaceae	Diploid	Heterosporous	Li et al. 2018	-	-	-	-	-
Marsilea vestita	Marsileaceae	Diploid	Heterosporous	-	Four studies*	-	-	-	-
Adiantum capillis-veneris	Pteridaceae	Diploid	Homosporous	-	-	Kawai-Tooyoka et al. 2004	-	Kawai et al. 2003	-
Pteris vittata	Pteridaceae	Tetraploid	Homosporous	-	-	-	Muthukumar et al. 2013	-	-
Ceratopteris richardii	Pteridaceae	Diploid	Homosporous	In progress	Stout et al. 2003	Rutherford et al. 2004	Muthukumar et al. 2013; Bui et al. 2015	Plackett et al. 2014, 2015	-

*Klink and Wolniak, 2000, 2001, 2003; Tsai and Wolniak 2001

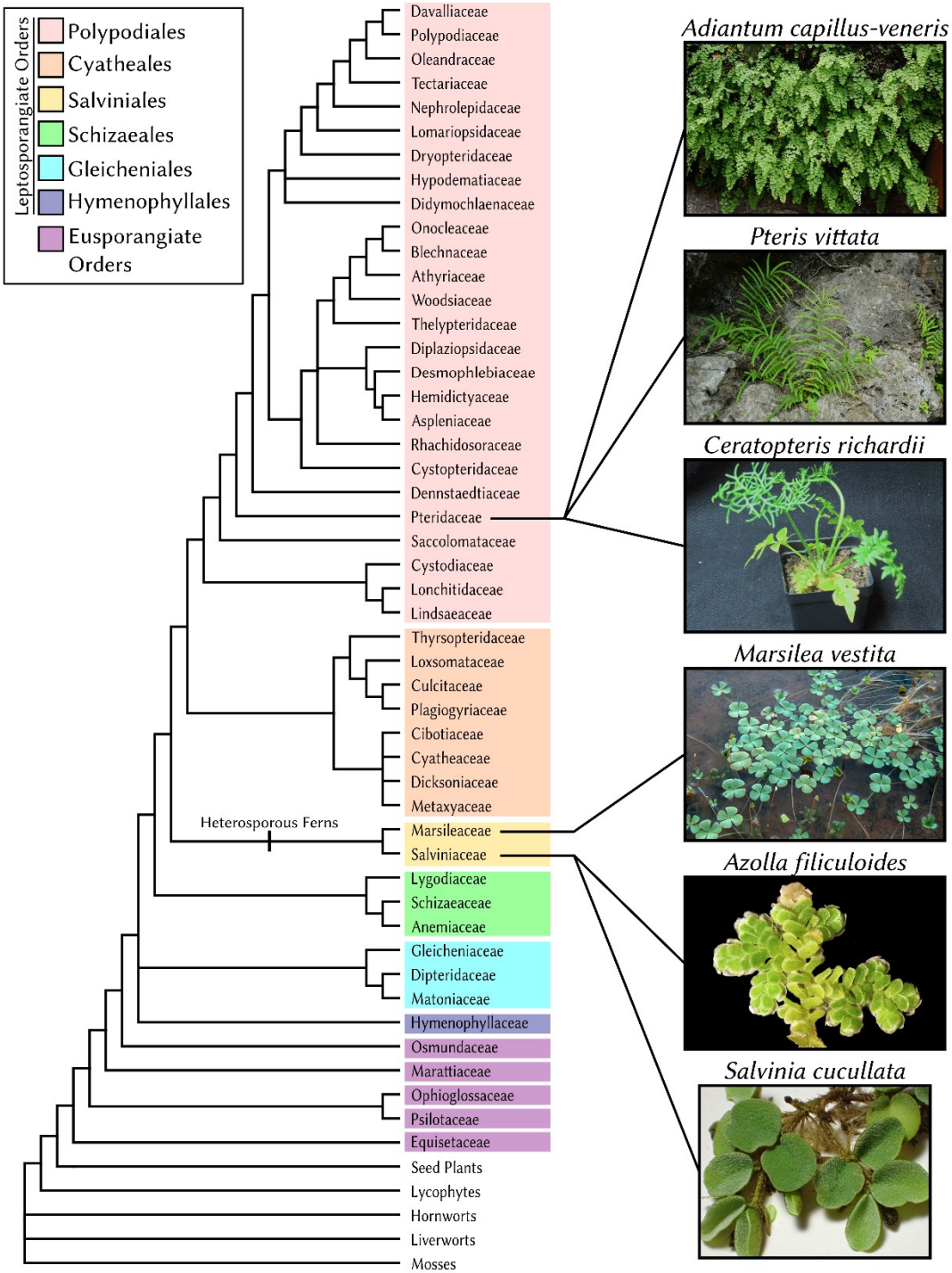

Figure 3.1 Phylogeny of fern families, highlighting prospective models. Photo credits: Pi-Fong Lu (*A. capillus-veneris*, *P. vittata*, and *S. cucullata*), Chi-Lien Cheng (*C. richardii*), Wikimedia Commons (*M. vestita*).

Azolla is well known for housing an obligate, vertically transmitted nitrogen-fixing cyanobacterium (*Nostoc azollae*) within specialized leaf cavities. Because of this symbiosis, *Azolla* has been used for over 1,000 years to fertilize rice paddies in Southeastern Asia (Lumpkin and Plucknett, 1980). Additionally, due to its fast growth rate and high protein content, *Azolla* has been used as supplementary feed for poultry (Basak *et al*., 2002), fish (Abou *et al*., 2007), and livestock (Cherryl *et al*., 2013). *Azolla* has also been investigated as a means to treat wastewater contaminated with pollutants like arsenic (Leão *et al*., 2017), synthetic textile dyes (Kooh *et al.*, 2016a, 2016b), swine waste (Muradov *et al*., 2014), fluoride (Zazouli *et al.*, 2014), excess nitrogen and phosphorus (Forni *et al*., 2001), and zinc (Zhao *et al*., 1999). Finally, using *Azolla* as a biofuel has been pursued as extracted lipids are suitable for the synthesis of biodiesel and meet requirements on fuel density, cetane number, and iodine value (Brouwer *et al*., 2016; Salehzadeh, Maeemi and Arasteh, 2014).

Salvinia plants grow in large mats, lack roots, have two floating leaves and a highly dissected, submerged leaf, which bears clusters of sori (Nagalingum, Schneider, and Pryer, 2006; Nagalingum, Nowak, and Pryer, 2008). In contrast to *Azolla*'s reputation as a generally beneficial plant, *Salvinia* is most well known as a noxious weed. With the exception of some limited research into the phytoremediation capacity of *Salvinia* (Baral *et al*., 2009), much of the biological research concerning this genus has involved controlling its weedy tendency (Room *et al*., 1981; Room, 1990). In the materials sciences, *Salvinia* has garnered attention for its ability to retain air on its leaf surfaces (termed the ‘‘Salvinia Effect’’) by

means of a unique combination of hydrophilic patches on a highly hydrophobic surface (Barthlott et al., 2010).

Genomic resources.—*Azolla filiculoides* and *Salvinia cucullata* both are diploid and have relatively small genomes (0.75 Gb in *A. filiculoides* and 0.26 Gb in *S. cucullata*). They are the only two ferns for which genomes have been sequenced (Li *et al*., 2018). The assembled genomes have N50 contig sizes of 964.7 Kb for *A. filliculoides* and 719.8 Kb for S. *cucullata*. A high level of completeness was indicated for both assemblies by BUSCO (Benchmarking Universal Single-Copy Orthologs) assessment and Illumina read-mapping results. Li *et al.* (2018) identified 20,201 high confidence gene models in *A. filliculoides* and 19,914 in *S. cucullata* that were supported by transcripts or were significantly similar to other known plant proteins. Additionally, medium-coverage resequencing was done on five other *Azolla* species, laying the foundation for future pan-genome and trait association studies. Genomic and transcriptomic data are available at FernBase (www.fernbase.org), along with genome browsers and BLAST utilities.

Available tools and technologies.—Brouwer *et al*. (2014) described a series of methods for collecting *A. filiculoides* spores, spore germination and in vitro fertilization, and cryopreservation of fertilized megaspores with their *N. azollae* symbiont. Both *A. filiculoides* and *S. cucullata* are relatively easy to maintain by growing in water in a growth chamber or greenhouse.

Missing tools.—Currently no transformation method has been developed for this lineage. Past studies have shown that it is feasible to generate protoplasts and callus tissues from several *Azolla* (Redford *et al*., 1987; Sini, Smitha, and

Madhusoodanan, 2014) and *Salvinia* species (Nakamura and Maeda, 1994), which could be useful for future development of transformation methods. It should also be noted that sexual reproduction of *S. cucullata* is seldom observed in the lab environment, which is not ideal for a model system.

Assessment as a model fern.—Both *A. filiculoides* and *S. cucullata* lack significant resources required of a model organism. Although neither *A. filiculoides* nor *S. cucullata* are particularly representative of the fern lineage as a whole, *A. filiculoides* would make an excellent model for studying plant-bacterial symbioses.

3.3 Marsilea vestita

Marsileaceae represents the other family of heterosporous ferns, sister to Salviniaceae (Figure 3.1). *Marsilea*, sometimes called the ‘‘water clover,’’ is a cosmopolitan genus of about 50 species (Whitten, Jacono, and Nagalingum, 2012) of aquatic to amphibious perennial ferns, which spread by rhizomes that may be floating, creeping, or subterranean (Jacono and Johnson, 2006). One particular *Marsilea* species, *M. vestita*, has been the focus of diverse developmental studies. Yet, the exact taxonomic placement of *M. vestita* remains unclear (Whitten, Jacono, and Nagalingum, 2012). The leaves of *Marsilea* are unlike those of any other fern, consisting of four terminal leaflets in a cruciform arrangement borne on a petiole. It is the only group of ferns to exhibit true nyctinasty, or daily movement of leaf orientation (Minorsky, 2018). This leaf arrangement is in contrast to the closely related genera *Regnellidium* (with two leaflets) and *Pilularia* (with a highly reduced, filiform leaf) (Pryer and Hearn, 2009). The highly desiccation tolerant reproductive structures of *Marsilea*, called sporocarps, consist of a stalk (termed ‘‘peduncle,’’

‘‘stipe,’’ or ‘‘pedicel’’) and a sclerified wall surrounding bisporangiate sori (Nagalingum, Schneider and Pryer, 2006, 2007). *Marsilea vestita* has been used as a model to study its uniquely rapid process of spermatogenesis (Wolniak *et al*., 2011). Upon rehydration of a microspore, a microgametophyte develops endosporically and spermatogenesis completes within 12 hours, releasing 32 highly flagellated sperms. The pioneering work by Stephen Wolniak and colleagues has shown that the rapid development of microgametophytes relies on translating stored RNA from microspores, and there is little or no de novo gene transcription (Boothby *et al*., 2013). At different stages of microgametophyte development, specific pools of stored pre-mRNAs are spliced to remove introns and enable translation. Through RNAi silencing, it was further demonstrated that such stage-specific mRNA maturation is required for proper gametophyte development (Boothby *et al*., 2013; Wolniak *et al*., 2011). A similar process also likely underlies megagametophyte development in *M. vestita* (Kuligowski, Ferrand, and Chenou, 1991), but few follow-up studies have been done.

Available tools and technologies.—*Marsilea vestita* can be easily grown in a container of water in a growth chamber or greenhouse environment. The history of research on *M. vestita* has resulted in numerous tools that will be useful to its development as a model system. A number of methods have been developed to localize mRNA transcripts during microgametophyte development in *M. vestita* (Boothby and Wolniak, 2011; Deeb *et al*., 2010; Kuligowski, Ferrand, and Chenou, 1991; Tsai, Van Der Weele, and Wolniak, 2004; Van Der Weele, Tsai, and Wolniak, 2007). Most importantly, *M. vestita* was the first fern in which RNAi was applied to

manipulate gene expression (Klink and Wolniak, 2000, 2001, 2003; Tsai and Wolniak, 2001). This was done by directly incubating microspores in the double-stranded RNA solution. It is, however, unclear if the same approach can be readily applied in other tissue types, and whether the silencing effect can be passed beyond fertilization to the sporophyte generation.

Missing tools.—Although there are several RNA-sequencing datasets published (Boothby *et al.*, 2013; Tomei and Wolniak, 2016), no reference genome exists for *M. vestita*. Because the smallest Marsilea genome reported to date is only 1.34Gb (Li *et al*., 2018; Kuo and Li, 2019), sequencing and assembling the *M. vestita* genome would likely be easier than a large homosporous fern genome. It should be noted that the generation time (from spore to spore) of *M. vestita* is unclear, as most of the past research focused on spermatogenesis that does not require the completion of life cycle.

Assessment as a model fern.—Lacking genomic data is not a significant hurdle in the effort to make *M. vestita* a model fern. Given the interest in addressing fundamental questions of life cycle evolution using ferns, a model heterosporous fern would be highly desirable, even if it is not representative of the entire fern lineage. The numerous studies conducted on *M. vestita* spermatogenesis make it a good system for studying mechanisms of cell biology, as well as a promising candidate to become a model heterosporous fern.

3.4 Adiantum capillus-veneris

Adiantum is a cosmopolitan, homosporous genus of 225 species in the Pteridaceae, nested within the leptosporangiate ferns (Figure 3.1, Huiet *et al*., 2018;

PPG 1, 2016). Molecular analyses revealed that *Adiantum* is sister to the vittarioids (shoestring ferns), despite stark morphological and ecological differences (Pryer *et al*., 2016; Schuettpelz and Pryer, 2007). The sporophytes of *Adiantum* are terrestrial, shade-loving, and bear compound leaves which, when fertile, produce sporangia only on false indusia. *Adiantum* gametophytes are determinate and cordate, with a distinct midrib and broad wings. Vittarioid sporophytes, on the other hand, are epiphytic and have simple, strap-shaped leaves with sori borne on the lamina. Vittarioid gametophytes are indeterminate, strap shaped, exceptionally long-lived, and can reproduce asexually via gemmae. Additionally, it is likely that at least one genome duplication occurred in the vittarioids after splitting from *Adiantum* (Pryer *et al*., 2016). The stark morphological, ecological, and genomic differences that exist between these sister lineages make them ideal for comparative studies to elucidate the genetic mechanisms that control traits like leaf shape and determinate versus indeterminate growth of gametophytes. *Adiantum*, in particular *A. capillus-veneris*, is perhaps most notable because it has served as a model to study photobiology. Masamitsu Wada and colleagues have used *A. capillus-veneris* to make several breakthroughs in phototropism, polarotropism, and chloroplast movement (Doi and Shimazaki, 2008; Imaizumi, 2000; Doi, Wada, and Shimazaki, 2006; Tsuboi *et al*., 2012). Several photoreceptors have also been functionally characterized in detail, including neochrome, a phytochrome-phototropin chimeric receptor (Li and Mathews, 2016; Wada, 2013). In addition, the first complete fern plastome was generated from *A. capillus-veneris* (Wolf *et al.*, 2003), which was used

to study levels of RNA-editing in the chloroplast genome (Wolf, Rowe, and Hasebe, 2004).

Available tools and technologies.—It is possible to manipulate gene expression in *A. capillus-veneris* via both gene overexpression and silencing. Genetic transformation by particle bombardment has been developed for gametophyte tissues and has been applied to rescue photoreceptor mutants (Kawai *et al.*, 2003), as well as to localize gene expression in conjunction with GUS (Tsuboi *et al*., 2012). In addition, Kawai-Toyooka *et al*. (2004) showed that gene silencing can be achieved by bombarding gametophytes with double-stranded DNA instead of a traditional RNAi approach. This DNAi method can produce up to 90% gene silencing efficiencies.

Missing tools.—While an EST library from gametophytes (Yamauchi *et al*., 2005) and a leaf transcriptome (Qi *et al*., 2018) have been published, no whole genome sequence has yet been generated for *A. capillus-veneris*. The genome size is unknown, although likely to be around 4–6Gb based on the estimates from congeneric species (Bainard *et al.*, 2011; Kuo and Li, 2019).

Assessment as a model fern.—In terms of morphology, reproductive strategy, and habit, *A. capillus-veneris* is a good representative of the fern lineage. It has been a useful system to study fern photobiology, and could provide insights into fundamental evo-devo questions, especially in comparison with the vittarioids.

3.5 Pteris vittata

Pteris is also a homosporous, leptosporangiate fern in the Pteridaceae (Figure 3.1; PPG1, 2016). The genus has now been recovered as monophyletic and

represents one of the largest fern genera, containing three subgenera and 200–250 species distributed globally (Zhang and Zhang, 2018). This diversity is reflected in the breadth of anatomy and habitat in which *Pteris* species are found. In 2001, *Pteris vittata* was discovered to hyperaccumulate arsenic (as high as 1% dry weight; Ma *et al.*, 2001). Though some other species in *Pteris* have also been found to possess this ability, *P. vittata* is the most efficient (Luongo and Ma, 2005). Because of its potential for phytoremediation applications, much of the research conducted on *P. vittata* has focused on elucidating the mechanism of arsenic accumulation (Cesaro *et al*., 2015; Datta *et al*., 2017; Gu *et al*., 2018; reviewed in Xie *et al*., 2009). *Pteris vittata* gametophytes, in particular, were proposed as a model system for analyzing arsenic hyperaccumulation because the rapid growth rate, small size, ease of culture, and haploid genome are more conducive to research than the sporophytes (Gumaelius *et al*., 2004). A number of transporters from *P. vittata* have been identified that mediate arsenite uptake (DiTusa *et al.*, 2016; He *et al*., 2016; Indriolo *et al*., 2010). Moreover, expression of a *P. vittata* arsenite antiporter ACR3;1 was able to reduce arsenic accumulation in shoots of Arabidopsis and tobacco, demonstrating a potential application in crops (Chen *et al*., 2017).

Available tools and technologies.—To test the function of ACR3 in *P. vittata*, a gene knock-down method by RNAi was developed, in which the RNAi constructs were biolistically bombarded into gametophyte tissues (Indriolo *et al*., 2010). Muthukumar *et al.* (2013) later showed that stable transformation can be achieved by co-incubation of spores with *Agrobacterium tumefaciens*. The

transformation efficiency was reported to be around 0.05% (Muthukumar *et al*., 2013).

Missing tools.—There is not yet a genome sequence for *P. vittata*, nor is there any published information on its genome size. Additionally, it should be noted that *P. vittata* is predominantly a tetraploid, and diploid individuals have a restricted geographical distribution (Srivastava, Ranade, and Khare, 2007). Furthermore, there is a mixture of reproductive strategies in this species, including sexual and apomictic, along with a range of ploidy levels (Chao *et al.*, 2012). The identification and collection of a sexual diploid strain would be vital to the future development of *P. vittata* as a model. Finally, there is no published guideline or manual on how to grow and maintain *P. vittata* in the lab.

Assessment as a model fern.—*P. vittata* lacks two of the most fundamental aspects of a model organism: genomic data and diploid representatives. While its development as a model organism would provide unique insight into arsenic tolerance and accumulation, significant resources would have to be dedicated to filling these gaps.

3.6 Ceratopteris richardii

Ceratopteris is also a homosporous, leptosporangiate fern in the Pteridaceae, though the taxonomy within the genus remains somewhat unsettled (Marchant, 2019). Polyploids and interspecific hybrids appear to be common in this genus (Lloyd, 1974), and further systematic work is needed, especially if members of this genus are to be used as model organisms.

Ceratopteris has been dubbed ‘‘the Arabidopsis of the fern world’’ (Sessa *et al.*, 2014). It has emerged as the most promising fern model species, largely because it can be readily cultured and transformed in the lab. *Ceratopteris richardii* is a diploid (n=39) aquatic fern that has been identified from Africa, Southeastern Asia, Japan, Australia, Fiji, and the Hawaiian Islands, although its highest concentration is in the Americas. It grows as an annual with a short, upright rhizome and slender, dimorphic leaves and divergent branches. Its short generation time (the life cycle can be completed in about 120 days) and small size make it a convenient lab model. Mature sporophytes are only about 5cm tall and spread over a diameter of less than 3cm, and gametophytes are even smaller. Thus, large numbers of plants can be cultured in a small growth chamber or greenhouse, enabling mutant screens. Plants can be vegetatively propagated easily from buds found on senescing fronds. Additionally, protoplasts can be isolated from gametophytes, and can regenerate to produce cultures (Edwards and Roux, 1998). A single mature sporophyte can produce around one million spores (per plant), which can be stored and remain viable for years (Chatterjee and Roux, 2000). Furthermore, a fast-growing cultivar strain of *C. richardii*, marketed as the ‘‘C-fern,’’ has been used as an educational model for K-12 and undergraduate instruction (Renzaglia and Warne, 1995). The ‘‘C-fern express’’ (also marketed for classroom use), on the other hand, is *C. thalictroides* (L.) Brongn., a tetraploid species (Hickok, Warne, and Fribourg, 1995).

Ceratopteris richardii is capable of intra-gametophytic self fertilization, resulting in completely homozygous sporophyte offspring (Haufler *et al*., 2016). At least three homozygous strains have been established (Hickok, Warne, and Fribourg,

1995). The most commonly used strain is Hn-n, which came from a spore on an herbarium specimen collected in Cuba. Two other strains are D176 from Guyana and PhiN8 from Nicaragua; they differ in leaf morphology, spore number per sporangium, as well as antheridiogen response (Hickok, Warne, and Fribourg., 1995; McGrath *et al*., 1994). All *C. richardii* strains can be crossed with each other and yield fertile F1 progeny (Hickok, Warne, and Fribourg, 1995).

Ceratopteris richardii has enabled research on a wide variety of topics, including gametophyte development (Banks, 1999), cell wall development (Leroux *et al*., 2013), evo-devo (*e.g.,* Hasebe *et al.*, 1998; Sano *et al*., 2005; Plackett *et al*., 2018), and plant responses to gravity in space flight (Bushart *et al*., 2013; Edwards and Roux, 1998; Salmi and Roux, 2008; Salmi *et al*., 2011). *Ceratopteris richardii* gametophytes in particular have served as a model for elucidating mechanisms of sex determination in ferns. Several sex determination mutants have been identified (Banks, 1994; Banks, 1997a, 1997b; Eberle *et al*., 1995; Strain, Hass, and Banks, 2001), and studies have been conducted on the hormones involved in sex determination (Atallah and Banks, 2015) as well as the effects of light (Kamachi *et al*., 2004, 2007; Murata and Sugai, 2000; Spiro, Torabi, and Cornell, 2004) and the soil microbiome (Ganger *et al.*, 2019) on gametophyte development and sex determination.

Ceratopteris richardii spores are the largest recorded within the homosporous ferns (~70—150 um in diameter), making them useful for electrophysiological studies on signal transduction pathways, which could be complicated by multicellularity (Chatterjee and Roux, 2000; Chatterjee *et al*., 2000).

The development of genetically identical spores is easy to synchronize, which allows for study and manipulation of the direction of polarity and cell level gravity responses within the first 24 hours of gametophyte development (Chaterjee and Roux, 2000). In 1999, *C. richardii* became the first ever ‘‘space fern,’’ on board Space Shuttle Columbia as a part of the STS-93 shuttle mission (Roux *et al*., 2003). It was found that in the spaceflight environment, around 5% of the transcripts in the *C. richardii* cDNA microarray were differentially regulated (Salmi and Roux, 2008).

Two recent studies fully explore *C. richardii's* potential as a model organism. Bui *et al*. (2017) investigated the genetic basis of fern apogamy—a type of asexual reproduction where sporophytes develop directly from gametophyte somatic cells without fertilization. Using a combination of transcriptome-sequencing, in situ hybridization, gene overexpression, and RNAi knockdown, it was demonstrated that *C. richardii* AINTEGUMENTA is required for promoting apogamous sporophytes (Bui *et al*., 2017). The second study focused on testing the function of LEAFY homologs in *C. richardii* (Plackett *et al*., 2018). While LEAFY in flowering plants is a key transcription factor that marks floral meristems, its role in ferns has been unknown. Using a similar suite of tools to Bui *et al*. (2017), Plackett *et al.* (2018) showed that *C. richardii* LEAFY plays an important role in maintaining apical stem cells throughout both sporophyte and gametophyte development.

Available tools and technologies.—*Ceratopteris richardii* is by far the most genetically tractable fern system (Table 3.1). Early attempts to manipulate gene expression involved RNAi and DNA vector-based gene silencing (Rutherford *et al*.,

2004; Stout *et al*., 2003). More recently, stable transformation has been achieved for *C. richardii* and *C. thalictroides* (‘‘C-fern express’’) using *Agrobacterium*-mediated transformation (Bui *et al.*, 2015; Muthukumar *et al*., 2013) and particle bombardment (Plackett *et al*., 2014; Plackett, Rabbinowitsch, and Langdale, 2015). The efficiency can be as high as 87% for transient transformants and 2.6% for stable transformants (Bui *et al*., 2015). In addition, a genetic linkage map has been produced for *C. richardii* using 488 doubled haploid lines that were genotyped for 368 restriction fragment length polymorphisms, 358 amplified fragment length polymorphisms, and three isozyme markers (Nakazato *et al*., 2006). This has been used to conduct quantitative trait locus (QTL) analysis to study reproductive barriers in C. richardii (Nakazato *et al*., 2007).

Missing tools.—The 11.25 Gb genome of *C. richardii* has yet to be fully sequenced (Marchant, 2019). Low coverage (1.73X) genome skimming data have been published (Wolf *et al.*, 2015) and the publication of a partially assembled genome is imminent (Marchant *et al*., 2019).

Assessment as a model fern.—A multitude of useful techniques have been developed for *C. richardii*, and it serves as the most prominent and promising prospective model fern at this point.

3.7 Conclusions and Outlook

All of the species reviewed here have the potential to become a model fern, but they all currently lack significant components of a complete model system. A genome has only been fully sequenced for *Azolla filiculoides* and *Salvinia cucullata*, yet no transformation methods have been developed for them. The closely related

Marsilea vestita, on the other hand, lacks a genome, but extensive research has been conducted to develop RNAi methods for this species. If a genome were sequenced for *M. vestita*, which is likely to be one of the smallest genomes in ferns (Li *et al*., 2018; Kuo and Li, 2019), much of the foundational work has already been completed to make it a promising model heterosporous fern.

Adiantum capillus-veneris has served as a model to study fern photobiology and some transformation methods have been developed; however, the genome has also not been sequenced. Similarly, *Pteris vittata* has garnered attention for its potential in the phytoremediation of arsenic. Though an *Agrobacterium*-mediated transformation method has been developed for *P. vittata*, the lack of a genome sequence and diploid strain hinder its emergence as a model.

The most developed model fern remains *Ceratopteris richardii* (also see Marchant, 2019). It has served as a model fern to tackle the genetic basis of sex determination and apogamy, as well as to elucidate the major transitions in plant evolutionary development. Efficient transformation methods via *Agrobacterium* and particle bombardment have been developed, and as exemplified by two recent studies by Bui *et al*. (2017) and Plackett *et al*. (2018), such genetic tools are powerful to link genes to specific biological functions. Importantly, the robust transformation methods also pave the way for developing CRISPR/Cas9 gene editing capacity, which has yet to be achieved in ferns (Table 3.1). Nevertheless, the 11.25 Gb genome, though typical of ferns, is limiting the full potential of *C. richardii* as a model organism. Fortunately, with the rapid advancement of

sequencing technologies, we believe a complete *C. richardii* genome should be delivered in the near future.

It would, of course, be ideal to establish more than one model organism for ferns. *Marsilea vesitita* is diploid, easy to grow in the lab, has not only a small genome that would be easy to sequence, but also numerous developed transformation techniques. Though the generation time is unclear, we envision that *M. vestita* would be the next most readily developed model and would nicely complement the homosporous *C. richardii* to serve as a heterosporous fern model. While using *M. vestita* and *C. richardii* as models will certainly not represent the whole of fern diversity, uniting resources behind these two models will enable plant biologists to study both ferns and the greater trends in land plant evolution.

REFERENCES

Abou, Y., E.D. Fiogbé, and J.C. Micha. 2007. Effects of stocking density on growth, yield and profitability of farming Nile tilapia, *Oreochromis niloticus* L., fed *Azolla* diet, in earthen ponds. Aquaculture Research 38:595-604.

Atallah, N.M. and J.A. Banks. 2015. Reproduction and the pheromonal regulation of sex type in fern gametophytes. Frontiers in Plant Science 6:1-6.

Bainard, J.D., T.A. Henry, L.D. Bainard, and S.G. Newmaster. 2011. DNA content variation in monilophytes and lycophytes: Large genomes that are not endopolyploid. Chromosome Research 19:763-775.

Banks, J. A. 1994. Sex-determining genes in the homosporous fern *Ceratopteris*. Development 120:1949–1958.

Banks, J.A. 1997a. Sex determination in the fern *Ceratopteris*. Trends in Plant Science 2:175–180.

Banks, J.A. 1997b. The *TRANSFORMER* genes of the fern *Ceratopteris* simultaneously promote meristem and archegonia development and repress antheridia development in the developing gametophyte. Genetics 147:1885–1897.

Banks, J.A. 1999. Gametophyte development in ferns. Annual Review of Plant Physiology and Plant Molecular Biology 50:163–186.

Baral, S.S., N. Das, T.S. Ramulu, S.K. Sahoo, S.N. Das, and G.R. Chaudhury. 2009. Removal of Cr(VI) by thermally activated weed *Salvinia cucullata* in a fixed-bed column. Journal of Hazardous Materials 161:1427–1435.

Barthlott, W., T. Schimmel, S. Wiersch, K. Koch, M. Brede, M. Barczewski, S. Walheim, A. Weis, A. Kaltenmaier, A. Leder, and H.F. Bohn. 2010. The *Salvinia* paradox: superhydrophobic surfaces with hydrophilic pins for air retention under water. Advanced Materials 22:2325–2328.

Basak, B., M.A.H. Pramanik, M.S. Rahman, S.U. Tarafdar, and B.C. Roy. 2002. *Azolla* (*Azolla pinnata*) as a feed ingredient in broiler ration. International Journal of Poultry Science 1:29–34.

Boothby, T.C. and S.M. Wolniak. 2011. Masked mRNA is stored with aggregated nuclear speckles and its asymmetric redistribution requires a homolog of mago nashi. BMC Cell Biology 12:45.

Boothby, T.C., R.S. Zipper, C.M. Van der Weele, and S.M. Wolniak. 2013. Removal of retained introns regulates translation in the rapidly developing gametophyte of *Marsilea vestita*. Developmental Cell 24:517–529.

Boyce, C.K. 2005. The Evolutionary History of Roots and Leaves. Pp. 479–499, *in* N.M Holbrook and M. Zwieniecki (eds.), *Vascular Transport in Plants*. Elsevier Ltd.

Brouwer, P., A. Bräutigam, C. Külahoglu, A.O.E. Tazelaar, S. Kurz, K.G.J. Nierop, A. van der Werf, A.P.M. Weber, and H. Schluepmann. 2014. *Azolla* domestication towards a biobased economy? New Phytologist 202:1069–1082.

Brouwer, P., A. van der Werf, H. Schluepmann, G.J. Reichart, and K.G.J. Nierop. 2016. Lipid yield and composition of *Azolla filiculoides* and the implications for biodiesel production. Bioenergy Research 9:369–377.

Bui, L.T., A.R. Cordle, E.E. Irish, and C.L. Cheng. 2015. Transient and stable transformation of *Ceratopteris richardii* gametophytes. BMC Research Notes 8:1–10.

Bui, L.T., D. Pandzic, C.E. Youngstrom, S. Wallace, E.E. Irish, P. Szövényi, and C.L. Cheng. 2017. A fern *AINTEGUMENTA* gene mirrors *BABY BOOM* in promoting apogamy in *Ceratopteris richardii*. Plant Journal 90:122–132.

Bushart, T.J., A.E. Cannon, A. ul Haque, P. San Miguel, K. Mostajeran, G.B. Clark, D.M. Porterfield, and S.J. Roux. 2013. RNA-Seq analysis identifies potential modulators of gravity response in spores of *Ceratopteris* (Parkeriaceae): Evidence for modulation by calcium pumps and apyrase activity. American Journal of Botany 100:161–174.

Cesaro, P., C. Cattaneo, E. Bona, G. Berta, and M. Cavaletto. 2015. The arsenic hyperaccumulating *Pteris vittata* expresses two arsenate reductases. Science Reports 5:1–10.

Chao, Y., H. -Y. Liu, Y. -C. Chiang, and W.-L. Chiou. 2012. Polyploidy and speciation in *Pteris* (Pteridaceae). Journal of Botany.

Chatterjee, A., D.M. Porterfield, P.S. Smith, and S.J. Roux. 2000. Gravity-directed calcium current in germinating spores of *Ceratopteris richardii*. Planta 210:607–610.

Chatterjee, A. and S.J. Roux. 2000. *Ceratopteris richardii*: A productive model for revealing secrets of signaling and development. Journal of Plant Growth Regulation 19:284–289.

Chen, Y., C.Y. Hua, M.R. Jia, J.W. Fu, X. Liu, Y.H. Han, Y. Liu, B. Rathinasabapathi, Y. Cao, and L.Q. Ma. 2017. Heterologous expression of *Pteris vittata* arsenite antiporter PvACR3;1 reduces arsenic accumulation in plant shoots. Environmental Science and Technology 51:10387–10395.

Cherryl, D.M., R.M. Prasad, and P. Jayalaxmi. 2013. A study on economics of inclusion of *Azolla pinnata* in swine rations. International Journal of Agricultural Sciences and Veterinary Medicine 1:50–56.

Datta, R., P. Das, R. Tappero, P. Punamiya, E. Elzinga, S. Sahi, H. Feng, J. Kiiskila, and D. Sarkar. 2017. Evidence for exocellular arsenic in Fronds of *Pteris vittata*. Science Reports 7:1–8.

Deeb, F., C.M. van der Weele, and S.M. Wolniak. 2010. Spermidine is a morphogenetic determinant for cell fate specification in the male gametophyte of the water fern *Marsilea vestita*. Plant Cell 22:3678–3691.

DiTusa, S.F., E.B. Fontenot, R.W. Wallace, M.A. Silvers, T.N. Steele, A.H. Elnagar, K.M. Dearman, and A.P. Smith. 2016. A member of the Phosphate transporter 1 (Pht1) family from the arsenic-hyperaccumulating fern *Pteris vittata* is a high-affinity arsenate transporter. New Phytologist 209:762–772.

Doi, M., M. Wada, and K. Shimazaki. 2006. The fern *Adiantum capillus-veneris* lacks stomatal responses to blue light. Plant and Cell Physiology 47:748–755.

Doi, M. and K. Shimazaki. (2008). The stomata of the fern *Adiantum capillus-veneris* do not respond to CO_2 in the dark and open by photosynthesis in guard cells. Plant Physiology 147:922–930.

Duckett, J., and W. Pang. 2014. Sexual behaviour of the terrestrial fern *Platyzoma microphyllum* R.Br.: a morphogenetic look at the origins of heterospory. Proceedings of the Royal Society of Edinburgh. 86: 457.

Eberle, J., J. Nemacheck, C. Wen, M. Hasebe, and J.A. Banks. 1995. *Ceratopteris*: a model system for studying sex-determining mechanisms in plants. International Journal Plant Science 156:359–366.

Edwards, E.S. and S.J. Roux. 1998. Influence of gravity and light on the developmental polarity of *Ceratopteris richardii* fern spores. Planta 205:553–560.

Evrard, C. and C. Van Hove. 2004. Taxonomy of the American *Azolla* species (Azollaceae): a critical review. Systematics and Geography of Plants 74:301–318.

Farrar, D.R. 1967. Gametophytes of four tropical fern genera reproducing independently of their sporophytes in the Southern Appalachians, Science 155: 1266-1267.

Forni, C., J. Chen, L. Tancioni, and M.G. Caiola. 2001. Evaluation of the fern *Azolla* for growth, nitrogen and phosphorus removal from wastewater. Water Research 35:1592–1598.

Ganger, M.T., R. Hiles, H. Hallowell, L. Cooper, N. McAllister, D. Youngdahl, J. Alfieri, and S. J. Ewing. 2019. A soil bacterium alters sex determination and rhizoid development in gametophytes of the fern *Ceratopteris richardii*. AoB PLANTS 11:1-12.

Gerrienne, P. and P. Gonez. 2011. Early evolution of life cycles in embryophytes: A focus on the fossil evidence of gametophyte/sporophyte size and morphological complexity. Journal of Systematics and Evolution 49:1–16.

Gu, Y., Y. Wang, Y. Sun, K. Zhao, Q. Xiang, X. Yu, X. Zhang, and Q. Chen. 2018. Genetic diversity and characterization of arsenic-resistant endophytic bacteria isolated from *Pteris vittata*, an arsenic hyperaccumulator. BMC Microbiology 18:1–10.

Gumaelius, L., B. Lahner, D.E. Salt, and J.A. Banks. 2004. Arsenic hyperaccumulation in gametophytes of *Pteris vittata:* a new model system for analysis of arsenic hyperaccumulation. Plant Physiology 136:3198–3208.

Harrison, C.J., S.B. Coriey, E.C. Moylan, D.L. Alexander, R.W. Scotland, and J.A. Langdale. 2005. Independent recruitment of a conserved developmental mechanism during leaf evolution. Nature 434:509–514.

Hasebe, M., C.K. Wen, M. Kato, and J.A. Banks. 1998. Characterization of *MADS* homeotic genes in the fern *Ceratopteris richardii*. Proceedings of the National Academy of Sciences 96:6222–6227.

Haufler, C.H., K.M. Pryer, E. Schuettpelz, E.B. Sessa, D.R. Farrar, R. Moran, J.J. Schneller, J.E. Watkins, and M.D. Windham. 2016. Sex and the single gametophyte: Revising the homosporous vascular plant life cycle in light of contemporary research. Bioscience 66:928–937.

He, Z., H. Yan, Y. Chen, H. Shen, W. Xu, H. Zhang, L. Shi, Y.G. Zhu, and M. Ma. 2016. An aquaporin PvTIP4;1 from *Pteris vittata* may mediate arsenite uptake. New Phytologist 209:746–761.

Hetherington, A.J. and L. Dolan. 2018. Stepwise and independent origins of roots among land plants. Nature 561:235–238.

Hickok, L.G., T.R. Warne, and R.S. Fribourg. 1995. The biology of the fern *Ceratopteris* and its use as a model system. International Journal of Plant Sciences 156:332–345.

Huiet, L., F.W. Li, T.T. Kao, J. Prado, A.R. Smith, E. Schuettpelz, and K.M. Pryer. 2018. A worldwide phylogeny of *Adiantum* (Pteridaceae) reveals remarkable convergent evolution in leaf blade architecture. Taxon 67:488–502.

Imaizumi, T. 2000. Cryptochrome nucleocytoplasmic dstribution and gene expression are regulated by light quality in the fern *Adiantum capillus-veneris*. Plant Cell 12:81–96.

Indriolo, E., G. Na, D. Ellis, D.E. Salt, and J.A. Banks. 2010. A vacuolar arsenite transporter necessary for arsenic tolerance in the arsenic hyperaccumulating fern *Pteris vittata* is missing in flowering plants. Plant Cell 22:2045–2057.

Jacono, C.C. and D.M. Johnson, D.M. 2006. Water-clover ferns, *Marsilea*, in the Southeastern United States. Castanea 71:1–14.

Kamachi, H., E. Matsunaga, M. Noguchi, and H. Inoue. 2004. Novel mutant phenotypes of a dark-germinating mutant *dkg1* in the fern *Ceratopteris richardii*. Journal of Plant Research 117:163–170.

Kamachi, H., O. Iwasawa, L.G. Hickok, M. Nakayama, M. Noguchi, and H. Inoue. 2007. The effects of light on sex determination in gametophytes of the fern *Ceratopteris richardii*. Journal of Plant Research 120:629–634.

Kawai, H., T. Kanegae, S. Christensen, T. Kiyosue, Y. Sato, T. Imaizumi, A. Kadota, and M. Wada. 2003. Responses of ferns to red light are mediated by an unconventional photoreceptor. Nature 421:287–290.

Kawai-Toyooka, H., C. Kuramoto, K. Orui, K. Motoyama, K. Kikuchi, T. Kanegae, and M. Wada. 2004. DNA interference: a simple and efficient gene-silencing system for high-throughput functional analysis in the fern. Plant Cell Physiology 45:1648–1657.

Klekowski, E. 1972. Genetical features of ferns as contrasted with seed plants. *Annals of the Missouri Botanical Garden* 59: 138–151.

Klekowski, E.J. and H.G. Baker. 1966. Evolutionary significance of polyploidy in the Pteridophyta. Science 153: 305-307.

Klink, V.P. and S.M. Wolniak. 2000. The efficacy of RNAi in the study of the plant cytoskeleton. Journal of Plant Growth Regulation 19:371–384.

Klink, V.P. and S.M. Wolniak. 2001. Centrin is necessary for the formation of the motile apparatus in spermatids of *Marsilea*. Molecular Biology of the Cell 12:761–776.

Klink, V.P. and S.M. Wolniak. 2003. Changes in the abundance and distribution of conserved centrosomal, cytoskeletal and ciliary proteins during spermiogenesis in *Marsilea vestita*. Cell Motility and the Cytoskeleton 56:57–73.

Kooh, M.R.R., M.K. Dahri, L.B.L. Lim, and L.H. Lim. 2016a. Batch Adsorption Studies on the Removal of Acid Blue 25 from Aqueous Solution Using *Azolla pinnata* and Soya Bean Waste. Arabian Journal for Science and Engineering 41:2453–2464.

Kooh, M.R.R., M.K. Dahri, L.B.L. Lim, and L.H. Lim. 2016b. Separation of toxic rhodamine B from aqueous solution using an efficient low-cost material, *Azolla pinnata*, by adsorption method. Environmental Monitoring and Assessment 188:1–15.

Kuligowski, J., M. Ferrand, and E. Chenou. 1991. Stored mRNA in early embryos of a fern *Marsilea vestita*: A paternal and maternal origin. Molecular Reproduction and Development 30:27–33.

Kuo, L.-Y., F.-W. Li. 2019. A roadmap for fern genome sequencing. American Fern Journal. in review.

Leão, G.A., J.A. de Oliveira, R.T.A. Felipe, and F.S. Farnese. 2017. Phytoremediation of arsenic-contaminated water: the role of antioxidant metabolism of *Azolla caroliniana* Willd. (Salviniales). Acta Botanica Brasilica 31:161–168.

Leroux, O., S. Eeckhout, R.L.L. Viane, and Z.A. Popper. 2013. *Ceratopteris richardii* (C-fern): a model for investigating adaptive modification of vascular plant cell walls. Frontiers in Plant Science 4:1–8.

Li, F.W., P. Brouwer, L. Carretero-Paulet, S. Cheng, J. de Vries, P.M. Delaux, A. Eily, M. Koppers, L.Y. Kuo, Z. Li, M. Simenc, I. Small, E. Wafula, S. Angarita, M. S. Barker, A. Brautigam, C.dePamphilis, S. Gould, P.S. Hosmani, Y.M.Huang, B. Huettel, Y. Kato, X. Liu, S. Maere, R. McDowell, L. A. Mueller, K.G.J. Nierop, S.A. Rensing, T. Robinson, C.J. Rothfels, E.M. Sigel, Y. Song, P.R. Timilsena, Y. V. de Peer, H. Wang, P.K.I Willhelmsson, P.G. Wolf, X, Xu, J.P. Der, H. Schluepmann, G.K.S. Wong, and K.M. Pryer. 2018. Fern genomes elucidate land plant evolution and cyanobacterial symbioses. Nature Plants 4:460–472.

Li, F.W. and S. Mathews. 2016. Evolutionary aspects of plant photoreceptors. Journal of Plant Research 129:115–122.

Lloyd, R.M. 1974. Systematics of the Genus *Ceratopteris* Brongn. (Parkeriaceae) II. Taxonomy. Brittonia 26:139–160.

Lumpkin, T.A. and D.L. Plucknett. 1980. *Azolla*: botany, physiology, and use as a green manure. Economic Botany 34:111–153.

Luongo, T. and L.Q. Ma. 2005. Characteristics of arsenic accumulation by *Pteris* and non-*Pteris* ferns. Plant Soil 277:117–126.

Ma, L.Q., K.M. Komar, C. Tu, W. Zhang, Y. Cai, and E.D. Kennelley. 2001. A fern that hyperaccumulates arsenic. Nature 409:579–579.

Marchant, D.B. 2019. Ferns with benefits: the incorporation of *Ceratopteris* into the genomics era. American Fern Journal 109(3):183—191.

McGrath, J.M., L.G. Hickok, and E. Pichersky. 1994. Restriction fragment length polymorphisms distinguish among accessions of *Ceratopteris thalictroides* and *C. richardii* (Parkeriaceae). Plant Systematics and Evolution 189:193–202.

Metzgar, J.S., H. Schneider, and K.M. Pryer. 2007. Phylogeny and divergence time estimates for the fern genus *Azolla* (Salviniaceae). International Journal of Plant Sciences 168:1045–1053.

Minorsky, P. V. 2018. The functions of foliar nyctinasty: a review and hypothesis. Biological Reviews. 94:216—229.

Muradov, N., M. Taha, A.F. Miranda, K. Kadali, A. Gujar, S. Rochfort, T. Stevenson, A.S. Ball, and A. Mouradov. 2014. Dual application of duckweed and *Azolla* plants for wastewater treatment and renewable fuels and petrochemicals production. Biotechnology and Biofuels 7:97–112.

Murata, T. and M. Sugai. 2000. Photoregulation of asymmetric cell division followed by rhizoid development in the fern *Ceratopteris* prothalli. Plant Cell Physiology 41:1313–1320.

Muthukumar, B., B.L Joyce, M.P. Elless, and C.N. Stewart. 2013. Stable transformation of ferns using spores as targets: *Pteris vittata* and *Ceratopteris thalictroides*. Plant Physiology 163:648–658.

Nagalingum, N.S., H. Schneider, and K.M. Pryer. 2006. Comparative morphology of reproductive structures in heterosporous water ferns and a reevaluation of the sporocarp. International Journal of Plant Sciences 167:805–815.

Nagalingum, N.S., H. Schneider, and K.M. Pryer. 2007. Molecular phylogenetic relationships and morphological evolution in the heterosporous fern genus *Marsilea*. Systematic Botany 32:16–25.

Nagalingum, N.S., M.D. Nowak, and K.M. Pryer. 2008. Assessing phylogenetic relationships in extant heterosporous ferns (Salviniales), with a focus on *Pilularia* and *Salvinia*. Botanical Journal of the Linnean Society 157:673–685.

Nakamura, M. and M. Maeda. 1994. Isolation and culture of protoplasts from young sporophytes of *Salvinia natans* aseptically obtained by co-culture of female and male gametophytes. Plant Cell, Tissue, and Organ Culture 36:237–242.

Nakazato, T., M.K. Jung, E.A. Housworth, L.H. Rieseberg, and G.J. Gastony. 2006. Genetic map-based analysis of genome structure in the homosporous fern *Ceratopteris richardii*. Genetics 173:1585–1597.

Nakazato, T., M.K. Jung, E.A. Housworth, L.H. Rieseberg, and G.J. Gastony. 2007. A genomewide study of reproductive barriers between allopatric populations of a homosporous fern, *Ceratopteris richardii*. Genetics 177:1141–1150.

Plackett, A.R.G., L. Huang, H.L. Sanders, and J.A. Langdale. 2014. High-efficiency stable transformation of the model fern species *Ceratopteris richardii* via microparticle bombardment. Plant Physiology 165:3–14.

Plackett, A.R.G., E.H. Rabbinowitsch, and J.A. Langdale. 2015. Protocol: Genetic transformation of the fern *Ceratopteris richardii* through microparticle bombardment. Plant Methods 11:1–10.

Plackett, A.R.G., S.J. Conway, K.D.H. Hazelton, E.H. Rabbinowitsch, J.A. Langdale, and V.S. Di Stilio. 2018. *LEAFY* maintains apical stem cell activity during shoot development in the fern *Ceratopteris richardii*. eLife. 7:e39625.

PPG I. 2016. A community-derived classification for extant lycophytes and ferns. Journal of Systematics and Evolution 54:563–603.

Pryer, K.M. and D.J. Hearn, D.J. 2009. Evolution of leaf form in Marsileaceous ferns: Evidence for heterochrony. Evolution 63:498–513.

Pryer, K.M., L. Huiet, F.W. Li, C.J. Rothfels, and E. Schuettpelz. 2016. Maidenhair ferns, *Adiantum*, are indeed monophyletic and sister to shoestring ferns, vittarioids (Pteridaceae). Systematic Botany 41:17–23.

Qi, X. L.Y. Kuo, C. Guo, H. Li, Z. Li, J. Qi, L. Wang, Y. Hu, J. Xiang, C. Zhang, J. Guo, C.H. Huang, H. Ma. 2018. A well-resolved fern nuclear phylogeny reveals the evolution history of numerous transcription factor families. Molecular Phylogenetics and Evolution 127:961–977.

Qiu, Y.L., A.B. Taylor, and H.A. McManus. 2012. Evolution of the life cycle in land plants. Journal of Systematics and Evolution 50:171–194.

Redford, K., M.D. Berliner, J.E. Gates, R.W. Fisher, and B.F. Matthews. 1987. Protoplast induction from sporophyte tissues of the heterosporous fern *Azolla*. Plant Cell, Tissue, and Organ Culture 10:187–196.

Reid, J.D., G.M. Plunkett, and G.A. Peters. 2006. Phylogenetic relationships in the heterosporous fern genus *Azolla* (Azollaceae) based on DNA sequence data from three noncoding regions. International Journal of Plant Sciences 167:529–538.

Renzaglia, K.S. and T.R. Warne. 1995. *Ceratopteris* : an ideal model system for teaching plant biology. International Journal of Plant Sciences 156:385–392.

Room, P.M., K.L.S. Harley, I.W. Forno, and D.P.A. Sands. 1981. Successful biological control of the floating weed *Salvinia*. Nature 294:78–80.

Room, P.M. 1990. Ecology of a simple plant-herbivore system: Biological control of *Salvinia*. Trends in Ecology and Evolution 5:74–79.

Roux, S.J., A. Chatterjee, S. Hillier, and T. Cannon. 2003. Early development of fern gametophytes in microgravity. Advances in Space Research 31:215–220.

Rutherford, G., M. Tanurdzic, M. Hasebe, and J.A. Banks. 2004. A systemic gene silencing method suitable for high throughput, reverse genetic analyses of gene function in fern gametophytes. BMC Plant Biology 4:1–10.

Salehzadeh, A., A.S. Naeemi, and A. Arasteh. 2014. Biodiesel production from *Azolla filiculoides* (Water Fern). Tropical Journal of Pharmacology Research 13:957–960.

Salmi, M.L. and S.J. Roux. 2008. Gene expression changes induced by space flight in single-cells of the fern *Ceratopteris richardii*. Planta 229:151–159.

Salmi, M.L., A. ul Haque, T.J. Bushart, S.C. Stout, S.J. Roux, and D.M. Porterfield. 2011. Changes in gravity rapidly alter the magnitude and direction of a cellular calcium current. Planta 233:911–920.

Sano, R., C.M. Juárez, B. Hass, K. Sakakibara, M. Ito, J.A. Banks, and M. Hasebe. 2005. *KNOX* homeobox genes potentially have similar function in both diploid unicellular and multicellular meristems, but not in haploid meristems. Evolution and Development 7:69–78.

Schuettpelz, E. and K.M. Pryer. 2007. Fern phylogeny inferred from 400 leptosporangiate species and three plastid genes. Taxon 56:1037–1050.

Sessa, E.B., J.A. Banks, M.S. Barker, J.P. Der, A.M. Duffy, S.W. Graham, M. Hasebe, J. Langdale, F.W. Li, D.B. Marchant, K.M. Pryer, C.J. Rothfels, S.J. Roux, M.L. Salmi, E.M. Sigel, D.E. Soltis, P.S. Soltis, D.W. Stevenson, P.G. Wolf. 2014. Between two fern genomes. Gigascience 3:1–7.

Sessa, E.B. and J.P. Der. 2016. Evolutionary Genomics of Ferns and Lycophytes. Pp. 215–254, *in* S.A. Rensing (ed.), *In Advances in Botanical Research*. Elsevier Ltd.

Sini, S., R.B. Smitha, and P.V. Madhusoodanan. 2014. Induction of sporocarp development in vitro in the mosquito fern, *Azolla rubra* R. Br. Annals of Plant Sciences 4:994–1002.

Spiro, M.D., B. Torabi, and C.N. Cornell. 2004. Cytokinins induce photomorphogenic development in dark-grown gametophytes of *Ceratopteris richardii*. Plant Cell Physiology 45:1252–1260.

Srivastava, J., S.A. Ranade, and P.B. Khare. 2007. Distribution and threat status of the cytotypes of *Pteris vittata* L. (Pteridaceae) species complex in India. Current Science 93:81–84.

Stout, S.C., G.B. Clark, S. Archer-Evans, and S.J. Roux. 2003. Rapid and efficient suppression of gene expression in a single-cell model system, *Ceratopteris richardii*. Plant Physiology 1:1165–1168.

Strain, E., B. Hass, and J.A. Banks. 2001. Characterization of Mutations that Feminize Gametophytes of the Fern *Ceratopteris*. Genetics 159:1271–1281.

Tomei, E.J. and S.M. Wolniak. 2016. Transcriptome analysis reveals a diverse family of kinesins essential for spermatogenesis in the fern *Marsilea*. Cytoskeleton 73:145–159.

Tryon, A.F. and F. Vida. 1967. *Platyzoma*: a new look at an old link in ferns. Science 156: 1109-1110.

Tsai, C.W. and S.M. Wolniak. 2001. Cell cycle arrest allows centrin translation but not basal body formation during spermiogenesis in *Marsilea*. Journal of Cell Science 114:4265–4272.

Tsai, C.W., C.M. Van Der Weele, and S.M. Wolniak. 2004. Differential segregation and modification of mRNA during spermiogenesis in *Marsilea vestita*. Developmental Biology 269:319–330.

Tsuboi, H., S. Nakamura, E. Schäfer, and M. Wada. 2012. Red light-induced phytochrome relocation into the nucleus in *Adiantum capillus-veneris*. Molecular Plant 5:611–618.

Van Der Weele, C.M., C.W. Tsai, and S.M. Wolniak. 2007. Mago nashi is essential for Spermatogenesis in *Marsilea*. Molecular Biology Cell 18:986–994.

Wada, M. 2013. Recent advances in the understanding of fern responses to light. Fern Gazette 19:97–115.

Wagner, G.M. 1997. *Azolla*: a review of its biology and utilization. Botanical Review 63:1–26.

Whitten, W.M., C.C. Jacono, and N.S. Nagalingum. 2012. An expanded plastid phylogeny of *Marsilea* with emphasis on North American species. American Fern Journal 102:114–135.

Wolf, P.G., C.A. Rowe, R.B. Sinclair, and M. Hasebe. 2003. Complete nucleotide sequence of the chloroplast genome from a leptosporangiate fern, *Adiantum capillus-veneris* L . DNA Research 65:59–65.

Wolf, P.G., C.A. Rowe, and M. Hasebe. 2004. High levels of RNA editing in a vascular plant chloroplast genome: Analysis of transcripts from the fern *Adiantum capillus-veneris*. Gene 339:89–97.

Wolf, P.G. E.B. Sessa, D.B. Marchant, F.W. Li, C.J. Rothfels, E.M. Sigel, M.A. Gitzendanner, C. J. Visger, J.A. Banks, D.E. Soltis, P.S. Soltis, K.M. Pryer, J.P. Der. 2015. An exploration into fern genome space. Genome Biology and Evolution 7:2533–2544.

Wolniak, S.M., C.M. van der Weele, F. Deeb, T. Boothby, and V.P. Klink. 2011. Extremes in rapid cellular morphogenesis: Post-transcriptional regulation of spermatogenesis in *Marsilea vestita*. Protoplasma 248:457–473.

Xie, Q.E., X.L. Yan, X.Y. Liao, and X. Li. 2009. Critical review the arsenic hyperaccumulator fern. Environmental Science and Technology 43:8488–8495.

Yamauchi, D., K. Sutoh, H. Kanegae, T. Horiguchi, K. Matsuoka, H. Fukuda, and M. Wada. 2005. Analysis of expressed sequence tags in prothallia of *Adiantum capillus-veneris*. Journal of Plant Research 118:223–227.

Zazouli, M.A., A.H. Mahvi, S. Dobaradaran, M. Barafrashtehpour, Y. Mahdavi, and D. Balarak. 2014. Adsorption of fluoride from aqueous solution by modified *Azolla filiculoides*. Fluoride 47:349–358.

Zhang, L. and L.B. Zhang. 2018. Phylogeny and systematics of the brake fern genus *Pteris* (Pteridaceae) based on molecular (plastid and nuclear) and morphological evidence. Molecular Phylogenetics and Evolution 118:265–285.

Zhao, M., J.R. Duncan, and R.P. Van Hille. 1999. Removal and recovery of zinc from solution and electroplating effluent using *Azolla filiculoides*. Water Research 33:1516–1522.

APPENDICES

APPENDIX 1: CTAB DNA extraction protocol

1 mL of CTAB extraction buffer (2% CTAB, 2% PVP-40, 1.4M NaCl; 20mM EDTA; 100mM Tris) with 1µL of β-mercaptoethanol at 65°C was added to each tube. Tubes were vortexed gently and incubated at 65°C for 20 minutes to 1 hour. Then 750 µL of 24:1 chloroform:isopentanol were added to each tube and mixed by inversion on a hula mixer for 5 minutes. Tubes were centrifuged for 5 minutes at 17000G and the aqueous layer was transferred to new tubes and the chloroform:isopentanol extraction was repeated once. The amount of remaining aqueous solution in each tube was then estimated and an equal amount of chilled isopropanol was added. Tubes were inverted thoroughly and centrifuged for 30 minutes at 21000G and 4°C. The supernatant was discarded and 1mL of chilled 70% ethanol was added to each tube. Tubes were then centrifuged for 5 minutes at 21000G and 4°C and the supernatant was discarded. This ethanol wash was repeated once. Resultant pellets were allowed to dry and were then resuspended in 50-100µL of Tris-HCl pH=7.5 and treated with RNAse.

APPENDIX 2: Fungal PCR protocol

Master mix recipe, per reaction: 11.85 µL PCR water; 5µL GoTaq Flexi Buffer; 2.5 µL dNTP's (1mM each); 2.5 µL BSA; 1 µL ITS1F primer; 1µL LR3 primer; 0.15 µL GoTaq (Promega); 1 µL DNA sample.

Primer sequences:

ITS1F: 5' CTTGGTCATTTAGAGGAAGTAA 3'

LR3: 5' GGTCCGTGTTTCAAGAC 3'

Thermocycler protocol: (1) 98°C for 5 minutes; (2) 98°C for 1 minute; (3) 56°C for 30 seconds; (4) 72°C for 1 minute; (5) repeat steps (2), (3), and (4) 34 times; (6) 72°C for 10 minutes.

APPENDIX 3: Bacterial PCR protocol

Master mix recipe, per reaction: 12.85 µL PCR water; 5 µL 5x GoTaq Flexi buffer; 2.5 µL dNTP's (1mM each); 2.5 µL BSA; 1µL 27F primer; 1µL 1492Rl primer; 0.15 µL GoTaq (Promega).

Primer sequences:

27F: 5' AGAGTTTGATCMTGGCTCAG 3'

1492Rl: 5' GGTTACCTTGTTACGACTT 3'

Thermocycler protocol: (1) 95°C for 4 minutes; (2) 95°C for 1 minute; (3) 60°C for 30 seconds; (4) 72°C for 1 minute 45 seconds; (5) repeat steps (2), (3), and (4) nine times, reducing step (3) by 1°C each time; (6) 95°C for 1 minute; (7) 50°C for 30 seconds; (8) 72°C for 1 minute 45 seconds; (9) repeat steps (6), (7), and (8) 17 times; (10) 72°C for five minutes 40 seconds.

APPENDIX 4: Bacterial DNA extraction protocol

Subcultures were transferred to liquid media in 2mL tubes and were inverted on a hula mixer overnight. Resultant bacteria were centrifuged for two minutes at 12000G and the media was discarded. Bacterial pellets were resuspended in 510.3 µL of SET buffer and 56.7µL lysozyme (10mg/mL). Tubes were vortexed and incubated at 37°C for one hour. 30µL 10% SDS and 3 µL proteinase K (20mg/mL) were added to each tube. Tubes were vortexed and incubated for another hour at 37°C. Then 100µL 5M NaCl were added and the tubes were vortexed. 80µL of 10% CTAB in 0.7M NaCl was added, the tubes were vortexed thoroughly, and incubated for 10 minutes at 65°C. 800µL 24:1 chloroform:isopentanol were added and tubes were mixed by inversion on a hula mixer for five minutes. Tubes were centrifuged for 5 minutes at 17000G and the aqueous layer was transferred to new tubes. The chloroform:isopentanol extraction was repeated once. The amount of remaining aqueous solution in each tube was then estimated and an equal amount of chilled isopropanol was added. Tubes were inverted thoroughly and centrifuged for 30 minutes at 21000G and 4°C. The supernatant was discarded and 1mL of chilled 70% ethanol was added to each tube. Tubes were then centrifuged for 5 minutes at 21000G and 4°C and the supernatant was discarded. This ethanol wash was repeated once. Resultant pellets were allowed to dry and were then resuspended in 50-100µL of Tris-HCl pH=7.5 and treated with RNAse.

APPENDIX 5: Fungal OTU distribution (1 = present, 0 = absent)

Fungal species ID	*De. dendroideum* aerial shoot	*De. dendroideum* subterranean shoot	*De. dendroideum* subterranean root	*Di. digitatum* subterranean shoot	*H. lucidula* aerial shoot	*H. lucidula* subterranean shoot	*H. lucidula* subterranean root	*L. clavatum* aerial shoot	*L. clavatum* subterranean root	*S. annotinum* aerial shoot	*S. annotinum* subterranean shoot
Ascomycota											
Sordariomycetes											
Anthostomella leucospermi	0	0	0	0	0	0	1	0	0	0	0
Nemania serpens	0	0	0	0	1	0	0	0	0	1	0
Nemania sp. 1	0	0	0	0	0	0	0	0	0	0	1
Dothideomycetes											
Dothideomycetes sp. 1	1	0	0	0	0	0	0	0	0	1	0
Pleosporales sp. 1	0	0	0	0	1	0	0	1	0	0	0
Leotiomycetes											
Leotiomycetes sp. 1	0	1	0	1	0	0	0	1	0	1	1
Eurotiomycetes											
Penicillium sp. 1	0	0	0	0	0	1	0	0	0	0	0
Mucoromycota											
Mucoromycota sp. 1	0	0	1	0	0	0	0	0	0	0	0
Mucoromycetes											
Umbelopsis ramanniana	0	0	0	0	0	1	0	0	0	0	0
Basidiomycota											
Agaricomycetes											
Peniophora pini	0	0	0	0	0	0	0	0	0	1	0
Unidentifiable fungus 1	0	0	0	0	0	0	0	0	1	0	0
Unidentifiable fungus 2	1	0	0	0	0	0	0	0	0	0	0
Unidentifiable fungus 3	0	0	0	0	0	0	0	0	0	1	0
Unidentifiable fungus 4	0	0	0	0	1	0	0	0	0	0	0
Unidentifiable fungus 5	0	0	0	0	0	1	0	0	0	0	0

APPENDIX 6: Bacterial OTU distribution (1 = present, 0 = absent)

Bacteria Sp.	*De. dendroideum* aerial shoot	*De. dendroideum* subterranean root	*De. dendroideum* subterranean shoot	*Di. Digitatum* aerial shoot	*Di. digitatum* subterranean root	*Di. digitatum* subterranean shoot	*H. lucidula* aerial shoot	*H. lucidula* subterranean root	*H. lucidula* subterranean shoot	*L. clavatum* aerial shoot	*L. clavatum* subterranean root	*S. annotinum* aerial shoot	*S. annotinum* subterranean root	*S. annotinum* subterranean shoot
Acidovorax sp. 1	0	0	0	0	0	0	1	0	0	0	0	0	0	0
Allobranchiibius huperziae	0	0	0	0	0	0	0	0	0	0	0	1	0	0
Bacillaceae sp. 1	0	0	1	0	0	0	1	0	0	0	0	0	0	0
Bacillaceae sp. 2	0	0	0	0	1	0	0	0	1	0	0	1	0	0
Bacillales sp. 1	0	0	0	0	0	0	0	0	1	0	0	0	1	1
Bacillales sp. 2	0	0	0	0	0	0	1	0	0	0	0	0	0	0
Bacillales sp. 3	0	0	0	0	0	0	1	0	0	0	0	0	0	0
Bacillus mycoides	0	0	1	0	0	0	0	0	1	0	0	0	1	0
Bacillus sp. 1	1	1	1	0	1	1	1	0	1	1	1	1	1	1
Bacillus sp. 2	0	1	0	0	1	0	0	1	0	0	1	1	0	0
Bacillus sp. 3	0	0	1	0	0	0	0	0	0	0	1	0	0	0
Bacillus sp. 4	0	0	0	0	1	0	0	0	0	0	0	0	0	0
Bacillus sp. 5	0	0	0	0	0	1	0	0	0	0	0	0	0	0
Bacillus sp. 6	0	0	0	0	0	0	0	0	0	0	1	0	0	0
Burkholderiaceae sp. 1	0	0	0	0	0	0	1	0	0	0	0	0	0	0
Burkholderiaceae sp. 2	0	0	0	0	0	1	1	0	1	0	0	0	0	0
Burkholderiaceae sp. 3	0	0	0	0	0	0	0	0	1	0	0	0	0	0
Burkholderiaceae sp. 4	0	0	0	0	0	0	0	0	0	0	1	0	0	0
Cohnella sp. 1	0	1	0	0	0	0	0	0	1	0	1	1	0	0
Dyella sp. 1	0	0	0	0	0	0	0	0	0	0	1	0	0	0
Erwinia sp. 1	0	0	0	0	0	0	1	0	0	0	0	0	0	0
Lysinibacillus sp. 1	0	0	0	0	1	0	1	1	0	0	0	0	1	0
Methylobacterium sp. 1	0	0	0	0	0	0	1	0	0	1	0	0	0	0
Methylobacterium sp. 2	0	0	0	0	0	0	1	0	0	0	0	0	0	0

Methylobacterium sp. 3	0	0	0	0	0	0	0	0	1	0	0	0	0	0
Microbacteriaceae sp. 1	0	0	0	0	0	0	1	0	0	0	0	0	0	0
Microbacteriaceae sp. 2	0	0	0	0	0	0	1	0	0	0	0	0	0	0
Microbacteriaceae sp. 3	0	0	0	0	0	0	1	0	0	0	0	0	0	0
Mycobacterium sp. 1	0	0	0	0	0	0	1	0	1	0	1	0	0	1
Nocardiaceae sp. 1	0	0	0	0	0	0	1	0	0	0	0	0	0	0
Paenibacillaceae sp. 1	0	0	0	1	0	0	0	0	0	0	0	0	0	0
Paenibacillus eucommiae	0	0	1	0	0	0	0	0	0	0	0	0	0	0
Paenibacillus sp. 1	0	1	1	1	0	1	1	1	1	0	1	1	1	0
Paenibacillus sp. 2	0	0	1	0	0	0	0	0	0	0	1	0	1	0
Paenibacillus sp. 3	0	0	0	0	0	0	0	0	1	0	0	0	1	1
Paenibacillus sp. 4	0	0	0	0	1	0	0	0	0	0	0	0	0	0
Paenibacillus sp. 5	0	0	0	0	1	0	0	1	0	0	0	0	0	0
Paenibacillus sp. 6	0	0	0	0	0	0	0	0	0	0	0	1	0	0
Paenibacillus sp. 7	0	0	0	0	0	0	1	0	0	0	0	0	1	1
Paenibacillus sp. 8	0	0	0	0	0	0	0	0	0	0	0	0	1	0
Paenibacillus sp. 9	0	0	0	0	0	0	0	0	0	0	1	0	0	0
Pseudomonas sp. 1	0	0	0	0	0	0	1	0	0	0	0	0	0	1
Pseudomonas sp. 2	0	0	0	0	0	0	0	0	1	0	0	0	0	0
Pseudorhodoplanes sinuspersici	0	0	0	0	0	0	0	0	0	0	1	0	0	0
Rhizobiaceae sp. 1	0	0	0	0	1	1	0	0	0	1	1	0	0	0
Rhodanobacteriaceae sp. 1	0	0	0	0	0	0	0	0	0	0	1	0	0	0
Sanguibacter sp. 1	0	0	0	0	0	0	1	0	0	0	0	0	0	0
Sphingomonas sp. 1	0	0	0	0	0	0	1	0	0	0	0	0	0	0
Stenotrophomonas sp. 1	0	0	0	0	0	0	1	0	0	0	0	0	0	0
Streptomyces sp. 1	0	0	0	0	0	0	0	0	0	0	0	0	0	1
Unidentifiable Bacteria sp. 1	0	0	0	0	0	0	0	0	1	0	0	0	0	0
Unidentifiable Bacteria sp. 2	0	0	0	0	0	0	0	0	1	0	0	0	0	0

APPENDIX 7: Table of collection information for all samples for ddRAD-seq

ID	Labeled species	Latitude	Longitude	Elev.	Locality	Date coll.	Collector	Herbarium ID
ID-1	*D. dendroideum*	48.6167	-117.1	1041	Pend Oreille Co. WA	13-Aug-2003	Gray	ID000297
ID-2	*D. dendroideum*	48.6167	-116.9833	814	Bonner Co. ID	15-Jul-2003	Gray	ID000292
JC-1	*D. dendroideum*	48.2383	-78.2828	269	Quebec, Canada	6-Jul-2019	Yin	
JC-3	*D. dendroideum*	47.9867	-79.3025	308	Quebec, Canada	5-Jul-2019	Hernandez-Rodriguez	
JC-4	*D. dendroideum*	47.9867	-79.3025	308	Quebec, Canada	5-Jul-2019	Hernandez-Rodriguez	
JC-5	*D. dendroideum*	47.357	-71.536	734	Quebec, Canada	8-Jul-2019	Bell-Doyon	
JC-6	*D. dendroideum*	47.482	-71.554	708	Quebec, Canada	17-Jul-2019	Bell-Doyon	
MONTU-1	*D. dendroideum*	47.03387	-112.38695	1661	Lewis and Clark Co. MT	1-Aug-2018	Varga	165141
NY-1	*D. dendroideum*	41.06667	-75.5	570	Monroe Co. PA	5-Oct-2005	Nee	3148212
NY-2	*D. dendroideum*	46.03833	-89.4422	540	Plum Lake, WI	26-Apr-2002	Majestyk	3148213
NY-4	*D. dendroideum*	44.5742	-68.1297	70	Steuben, ME	22-Aug-2013	Matos	2696034
NY-5	*D. dendroideum*	44.8461	-70.66194	720	Franklin Co, ME	18-Jun-2007	Atha	1070818
VT-2	*D. dendroideum*	42.516	-74.149	465	Rensselaerville, NY	8-Jun-2014	Testo	UVMVT185451
VT-3	*D. dendroideum*	43.88	-73.66	358	Essex Co. NY	21-Apr-2014	Testo	UVMVT185442
VT-7	*D. dendroideum*			243	Duxbury VT	7-Sep-2002	Shustack	UVMVT025913
WTU-1	*D. dendroideum*	58.310278	-134.1175	14	Juneau Quad, AK	13-Jul-2012	Parker	WTU-V-029523
WTU-3	*D. dendroideum*	47.79005	-121.558807	597	Snohomish Co WA	11-Nov-2011	Legler	WTU-V-019872
WTU-4	*D. dendroideum*	54.9385	-131.3768	85	Duke Island, AK	26-Jun-2008	Stensvold	WTU-V-022767
WTU-5	*D. dendroideum*	47.03387	-112.38695	1923	Cadott Creek Quad, MT	1-Aug-2018	Varga	WTU-V-041247
WTU-6	*D. dendroideum*			220	Sakhalin Island, Russia	24-Aug-2003	Legler	WTU-V-040734

WTU-7.1	*D. dendroideum*	49.72972	142.52417	120	Sakhalin Island, Russia	26-Jul-2003	Legler	WTU-V-040762
WTU-7.2	*D. dendroideum*	49.72972	142.52417	120	Sakhalin Island, Russia	26-Jul-2003	Legler	WTU-V-040762
WTU-9	*D. dendroideum*	47.9983	142.89917	40	Sakhalin Island, Russia	17-Jul-2003	Legler	WTU-V-040733
ARP_0004	*D. dendroideum*	42.54805	-76.26628	326	McLean Bog	7-Nov-2018	Petlewski	N/A
ARP_0014	*D. dendroideum*	42.54909	-76.26700	326	McLean Bog	7-Nov-2018	Petlewski	N/A
ARP_0018	*D. dendroideum*	42.54913	-76.26692	326	McLean Bog	7-Nov-2018	Petlewski	N/A
ARP_0031A	*D. dendroideum*	42.35537	-76.37257	554	Bald Hill	2-May-2019	Petlewski	N/A
ARP_0033E	*D. dendroideum*	42.33707	-76.33904	454	Shindagin	2-May-2019	Petlewski	N/A
ARP_0033F	*D. dendroideum*	42.33707	-76.33904	454	Shindagin	2-May-2019	Petlewski	N/A
ARP_0033H	*D. dendroideum*	42.33707	-76.33904	454	Shindagin	2-May-2019	Petlewski	N/A
BH-5	*D. dendroideum*	44.89166	-68.06472	200	Lead Mtn, Hancock ME	23-Aug-2013	Choo	BH 000 077 103
BRU-11	*D. hickeyi*	41.99632	-71.44208	135	Cumberland, RI	17-Aug-2016	Whitfeld	BRU 00056674
BRU-12	*D. hickeyi*	41.64618	-71.7495	134	West Greenwich, RI	8-Jun-2017	Whitfeld	BRU 00064143
BRU-13	*D. hickeyi*	42.006167	-71.435	103	Cumberland, RI	12-Jun-2018	Whitfeld	BRU 00066910
BRU-14	*D. hickeyi*	41.9965	-71.4444	139	Cumberland, RI	16-Sep-2016	Hecht	BRU 00051467
BRU-15	*D. hickeyi*	41.60167	-71.72667	52	Kent Co. RI	9-Oct-2015	Adams	BRU 00033455
BRU-7	*D. hickeyi*	48.15611	-91.79694	415	Lake Co, MN	17-Aug-2015	Whitfeld	BRU 00050362
BRU-8	*D. hickeyi*	48.19425	-91.97667	410	St. Louis Co. MN	31-Jul-2016	Whitfeld	BRU 00058361
BRU-9	*D. hickeyi*	41.54136	-71.590277	60	Washington Co, RI	15-Aug-2014	Whitfeld	BRU 00028149
CJR-5392	*D. hickeyi*	41.448	-71.5368	60	Washington Co, RI	19-Jun-2019	Rothfels	Duke Fern Lab #13847
JC-2	*D. hickeyi*	48.22917	-78.279	283	Quebec, Canada	4-Jul-2019	Yin	
NY-6	*D. hickeyi*	44.6077	-68.0381	70	Hancock Co. ME	19-Aug-2013	Matos	2696059

NY-7	*D. hickeyi*	44.47722	-73.57667	276	Clinton Co NY	25-Aug-2010	Naczi	3418300
NY-8	*D. hickeyi*	39.18972	-75.6483	12	Kent Co DE	19-Apr-2009	Naczi	3148354
VT-9	*D. hickeyi*			355	Cabot, VT	10-Jul-2002	Barrington	UVMVT067105
WTU-10	*D. hickeyi*	42.45	-71.342	45	Middlesex Co MA	20-Dec-2014	Zika	WTU-V-040827
WTU-11	*D. hickeyi*	43.0006	-72.52694	117	Franklin Co MA	17-Oct-2005	Legler	WTU-V-040749
WTU-12	*D. hickeyi*	42.45	-71.342	45	Middlesex Co MA	20-Dec-2014	Sika	WTU-V-017135
NY-39	*D. juniperoideum*	52.35472	143.0083	15	Sakhalin Island, Russia	4-Aug-2003	Legler	3831738
NY-40	*D. juniperoideum*	45.80139	149.9039	4	Urup, Russia	28-Aug-1995	Gage	3831742
NY-41	*D. juniperoideum*	49.7297	121.52416	120	Sakhalin Island, Russia	26-Jul-2003	Legler	3831746
WTU-2	*D. juniperoideum*	52.35472	143.0083	15	Sakhalin Island, Russia	4-Aug-2003	Legler	WTU-V-040763
LYK-1	*D. juniperoideum*			3275-3417	Hualien County, Taiwan	16-Aug-2010	Lu	Taiwan Forestry Research Institute 349236
BRU-1	*D. obscurum*	41.61241	-71.62111	104	Kent, RI	16-Sep-2017	Buhr	BRU 00024697
BRU-10	*D. obscurum*	41.874833	-71.320556	27	Seekonk, MA	22-Aug-2015	Johnson	BRU 00033454
BRU-4	*D. obscurum*	42.27583	-73.30417	329	Berkshire, MA	10-Jun-2015	Dunca	BRU 00036941
BRU-5	*D. obscurum*	41.53917	-71.152778	43	Newport Co, RI	29-Sep-2017	Burdo	BRU 00060266
BRU-6	*D. obscurum*	41.4775	-71.703611	39	Richmond, RI	28-Sep-2018	Mancini	BRU 00073456
NY-11	*D. obscurum*	41.180556	-73.58556	150	Westchester, NY	20-Jun-2013	Matos	1096861
NY-13	*D. obscurum*			0	Luzerne Co, PA	25-Jul-2007	Montgomery	3147990
NY-16	*D. obscurum*	39.96472	-74.9225	20	Burlington Co, NJ	12-Jan-2009	Longbottom	3148031
NY-22	*D. obscurum*	38.75861	-75.73194	11	Caroline Co, MD	5-Jan-2011	Longbottom	3148040

NY-23	*D. obscurum*	39.1425	-76.6622	30	Dunkirk, MD	20-Dec-2015	Longbottom	2902602
NY-28	*D. obscurum*	38.7361	-76.73167	12	Federalsburk, MD	3-Apr-2013	Longbottom	2200638
NY-29	*D. obscurum*	38.80583	-75.51278	20	Owens, DE	7-Feb-2009	Longbottom	3148058
NY-30	*D. obscurum*	39.5689	-75.7175	29	New Castle Co. DE	1-Jul-2011	Naczi	3148050
NY-34	*D. obscurum*	39.2767	-75.4822	9	Kent Co DE	13-Jan-2013	Longbottom	2219075
NY-36	*D. obscurum*	36.62543	-81.50143	1520	Grayson Co. VA	29-May-2008	Atha	1070863
NY-9	*D. obscurum*	44.46	-67.92861	200	Hancock Co. ME	23-Aug-2013	Matos	2696066
VT-10	*D. obscurum*	44.55	-73.28	32	Colchester VT	9-Sep-2012	Testo	UVMVT025001
VT-14	*D. obscurum*			32	South Burlington VT	21-Aug-2012	Testo	UVMVT025002
WTU-14	*D. obscurum*	46.9	143.05	40	Sakhalin Island, Russia	29-Jul-2001	Joneson	WTU-V-041812
WTU-15	*D. obscurum*	42.5006	-72.52694	117	Franklin Co MA	17-Oct-2005	Legler	WTU-V-041809
ARP_0007	*D. obscurum*	42.54796	-76.26634	326	McLean Bog	7-Nov-2018	Petlewski	N/A
ARP_0008	*D. obscurum*	42.54795	-76.26635	326	McLean Bog	7-Nov-2018	Petlewski	N/A
ARP_0009	*D. obscurum*	42.54793	-76.26635	326	McLean Bog	7-Nov-2018	Petlewski	N/A
ARP_0011	*D. obscurum*	42.54786	-76.26639	326	McLean Bog	7-Nov-2018	Petlewski	N/A
ARP_0016	*D. obscurum*	42.54908	-76.26699	326	McLean Bog	7-Nov-2018	Petlewski	N/A
ARP_0017	*D. obscurum*	42.54914	-76.26693	326	McLean Bog	7-Nov-2018	Petlewski	N/A
ARP_0019	*D. obscurum*	42.54932	-76.26673	326	McLean Bog	7-Nov-2018	Petlewski	N/A
ARP_0021	*D. obscurum*	42.54936	-76.26674	326	McLean Bog	7-Nov-2018	Petlewski	N/A
ARP_0022	*D. obscurum*	42.54943	-76.26679	326	McLean Bog	7-Nov-2018	Petlewski	N/A
ARP_0023	*D. obscurum*	42.54938	-76.26683	326	McLean Bog	7-Nov-2018	Petlewski	N/A
ARP_0032E	*D. obscurum*	42.35481	-76.37137	554	Bald Hill	2-May-2019	Petlewski	N/A
ARP_0032G	*D. obscurum*	42.35481	-76.37137	554	Bald Hill	2-May-2019	Petlewski	N/A
WTU-13	*D. sp.*	47.25	142.81667	91	Sakhalin Island, Russia	17-Jul-2001	Joneson	WTU-V-041811

ARP_0005	*D. sp.*	42.54795	-76.26633	326	McLean Bog	7-Nov-2018	Petlewski	N/A
ARP_0012	*D. sp.*	42.54901	-76.26702	326	McLean Bog	7-Nov-2018	Petlewski	N/A
ARP_0015	*D. sp.*	42.54901	-76.26703	326	McLean Bog	7-Nov-2018	Petlewski	N/A
ARP_0028A	*D. sp.*	42.35523	-76.37339	554	Bald Hill	2-May-2019	Petlewski	N/A
ARP_0029A	*D. sp.*	42.35524	-76.37324	554	Bald Hill	2-May-2019	Petlewski	N/A
ARP_0029D	*D. sp.*	42.35524	-76.37324	554	Bald Hill	2-May-2019	Petlewski	N/A
ARP_0032B	*D. sp.*	42.35481	-76.37137	554	Bald Hill	2-May-2019	Petlewski	N/A
ARP_0032C	*D. sp.*	42.35481	-76.37137	554	Bald Hill	2-May-2019	Petlewski	N/A
ARP_0032D	*D. sp.*	42.35481	-76.37137	554	Bald Hill	2-May-2019	Petlewski	N/A
ARP_0032H	*D. sp.*	42.35481	-76.37137	554	Bald Hill	2-May-2019	Petlewski	N/A
ARP_0025A	*D. sp.*	42.35536	-76.37320	554	Bald Hill	2-May-2019	Petlewski	N/A
DB-12556	*D. verticale*	29.54636	103.3365	2459	Mt. Emeishan, Sichuan, China	15-Jul-2017	Rothfels	Duke Fern Lab #12556
DB-12557	*D. verticale*	29.51657	103.33204	2991	Mt. Emeishan, Sichuan, China	15-Jul-2017	Rothfels	Duke Fern Lab #12557
ARP_0001	*Diphasiastrum digitatum*	42.54458	-76.26668	326	McLean Bog	7-Nov-2018	Petlewski	N/A
ARP_0033A	*Lycopodium clavatum*	42.33707	-76.33904	454	Shindagin	2-May-2019	Petlewski	N/A
ARP_0033D	*Spinulum annotinum*	42.33707	-76.33904	454	Shindagin	2-May-2019	Petlewski	N/A

APPENDIX 8: ddRAD-seq protocol

Digestion: For each sample, the following reagents were mixed in a PCR tube on ice: 10 µL DNA (or 500ng, whichever volume was greater); 1µL EcoRI (20,000 units/mL); 2µL MseI (10,000 units/mL); 5µL 10x CutSmart buffer (New England Biolabs); PCR water to a total volume of 50µL. Samples were incubated at 37°C for three hours, followed by 65°C for 10 minutes.

MseI oligo preparation: MseI oligos (Appendix 9) had to be annealed before ligation by combining 10µL MseI1 oligo (100µM stock), 10µL MseI2 oligo (100µM stock), and 80µL PCR water in a PCR tube. The tube was incubated with the following steps: (1) 95°C for 5 minutes; (2) 80°C for 30 seconds, looped 58 times with temperature reducing by 1°C each loop; (3) 22°C for 1 minute; (4) 95°C for 5 minutes; and (5) 80°C for 30 seconds, looped 58 times with the temperature reducing by 1°C each loop.

Ligation: For each sample, the following reagents were added to a PCR tube on ice: 2µL 10X T4 ligase buffer (New England Biolabs); 1µL prepared MseI adapter (10µM); 0.4µL T4 ligase (New England Biolabs); 3.6µL PCR water; 12µL digested DNA; and 1µL barcoded EcoRI adapter. Tubes were incubated at 23°C for 1 hour.

PCR: For each sample, the following reagents were added to a PCR tube on ice: 7.65 µl PCR water; 4µL 5x Phusion HF buffer (New England Biolabs); 4µL mixed dNTPs (1mM each); 2µL 2.5µM pooled IllPCR primers; 0.15µL DMSO; 0.2µL Phusion DNA polymerase (New England Biolabs); 2µL digested, ligated DNA product. Tubes were incubated in the following steps: (1) 98°C for 30

seconds; (2) 98°C for 20 seconds; (3) 60°C for 30 seconds; (4) 72°C for 40 seconds; loop steps (2), (3), and (4) 29 times; and (5) 72°C for 10 minutes.

APPENDIX 9: **ddRAD-seq primer and oligo sequences**

MseI1 oligo: 5' GCAGAAGACGGCATACGAGCTCTTCCCATCTG 3'

MseI2 oligo: 5' TACAGATCGGAAGAGCTCGTATGCCGTCTTCTGCTTG 3'

IllPCR1 oligo: 5' A*A*TGATACGGCGACCACCGAGATCTACACTCTTTCCCT ACACGACGCTCTTCCGATCT 3'

IllPCR2 oligo: 5' C*A*AGCAGAAGACGGCATACGAGCTCTTCCGATCTGT AAG 3'

*=phosphothiolated base